



Title	Antibacterial effects of a glass-ionomer cement incorporating bio-active fillers with acidity-induced zinc ion-releasing ability
Author(s)	Liu, Yuhan
Citation	大阪大学, 2021, 博士論文
Version Type	VoR
URL	https://doi.org/10.18910/85363
rights	
Note	

The University of Osaka Institutional Knowledge Archive : OUKA

<https://ir.library.osaka-u.ac.jp/>

The University of Osaka

**Antibacterial effects of a glass-ionomer cement
incorporating bio-active fillers
with acidity-induced zinc ion-releasing ability**

Osaka University Graduate School of Dentistry

Course for Oral Science

(Department of Biomaterials Science)

Supervisor: Professor Satoshi Imazato

Yuhan Liu

ACKNOWLEDGEMENT

Over the past four-year Ph.D. journey, so many people have helped me and made my life in Osaka an unforgettable experience. I am really grateful to all of you.

I would like to express my sincere appreciation to my supervisor, Professor Satoshi Imazato, Chair of the Department of Biomaterials Science, Osaka University Graduate School of Dentistry, for his guidance and supervision. He is a warm and extremely wise professor, every time after discussions I learned new knowledge and got valuable advice. On the other hand, he is an intelligent man who knows how to find a perfect balance between research work and life and always encourages and supports me throughout the years. I could learn not only scientific research but also his life attitude from him. I'm really thankful and feel lucky he accepted me as his student and thank you for being such an inspiring role model.

I would like extend to many thanks to Assistant Professor Haruaki Kitagawa for providing me valuable advice and a lot of support. Thank you so much for always reminding me to be critical and offering me invaluable hints at some critical moments of my thesis writing. During these years, I benefit from his guidance, comments, and encouragement. I truly appreciate your patience and support in instructing me.

The biggest thanks go to all the teachers and members in our department, thank you for the tips, advice, and encouragement along my Ph.D. journey. You have made my life in Osaka much easier at the beginning and truly enjoyable. Special thanks to all my

friends who have supported me, hosted me, and encouraged me. I also appreciate those many lunches, drinks, talks and discussions with my friends.

To my parents, thank you for understanding and supporting me in my decision to pursue a Ph.D. I am forever indebted to your endless love all these years, gratitude for the love and care.

To my husband, thanks for your love and understanding. You always support and stand by my side. I'm so lucky to meet you.

From eighteen, I spent twelve years bringing my doctoral thesis to show you, I'm glad that I did not quit and finally stuck with it. I'm not sure if it worth but hopefully, someone might be inspired by my dissertation. Life is always hard, especially under this COVID-19 pandemic. But what makes humans civilized is love, thank all the people surround me treat me as usual. Hope we could get through it soon and everyone will have a good future.

Finally, I appreciate China Scholarship Council for its financial assistance over the past three years.

Yuhan Liu

INDEX

GENERAL INTRODUCTION	1
OBJECTIVES AND CONTENTS	5
EXPERIMENT 1: Evaluation of Zn ²⁺ -release characteristic and antibacterial activity of BioUnion filler	
1.1 Materials and methods	6
1.1.1 Materials	
1.1.2 Characterization of BioUnion filler (BU)	
1.1.3 Evaluation of ion release from BU	
1.1.4 Measurement of MICs and MBCs of Zn ²⁺ , Ca ²⁺ , and F ⁻ for oral bacteria	
1.1.5 Evaluation of antibacterial activity of BU	
1.1.6 Evaluation of Zn ²⁺ -release from BU with repeated exposure to acid and inhibition of <i>S. mutans</i>	
1.2 Results	13
1.2.1 Characterization of BU	
1.2.2 Ion release from BU	
1.2.3 MICs and MBCs of Zn ²⁺ , Ca ²⁺ , and F ⁻ for oral bacteria	
1.2.4 Antibacterial activity of BU	
1.2.5 Zn ²⁺ -release from BU with repeated exposure to acid and inhibition of <i>S. mutans</i>	
1.3 Discussion	17
1.4 Summary	23

EXPERIMENT 2: Evaluation of Zn²⁺-release characteristic and antibacterial activity of a GIC containing BioUnion filler

2.1	Materials and methods	24
2.1.1	Materials	
2.1.2	Evaluation of ion release from the GIC containing BU (CA)	
2.1.3	Elemental analysis of CA	
2.1.4	Evaluation of antibacterial activity of CA	
2.1.5	Evaluation of bacterial adherence to CA	
2.1.6	<i>In situ</i> assessments of antibacterial effect of CA	
2.2	Results	32
2.2.1	Ion release from CA	
2.2.2	Elemental analysis of CA	
2.2.3	Antibacterial activity of CA	
2.2.4	Bacterial adherence to CA	
2.2.5	<i>In situ</i> assessments of antibacterial effect of CA	
2.3	Discussion	34
2.4	Summary	42

EXPERIMENT 3: Evaluation of physical properties and bonding ability of CA

3.1	Materials and methods	44
3.1.1	Setting time	
3.1.2	Acid erosion	
3.1.3	Compressive strength	

3.1.4	Toothbrush wear	
3.1.5	Bond strength to enamel and dentin	
3.2	Results	48
3.2.1	Setting time	
3.2.2	Acid erosion	
3.2.3	Compressive strength	
3.2.4	Toothbrush wear	
3.2.5	Bond strength to enamel and dentin	
3.3	Discussion	50
3.4	Summary	52
	GENERAL CONCLUSIONS	53
	REFERENCES	55
	TABLE AND FIGURE LEGENDS	73
	TABLES AND FIGURES	79

GENERAL INTRODUCTION

Dental caries, a major oral health problem worldwide, is caused by the formation of a cariogenic environment in the oral cavity and depends on many factors including diet and oral hygiene [1]. Moreover, people try to prevent/manage dental caries by overzealous toothbrushing, which could promote gingival recession [2] and elevate the risk of root surface caries in elderly individuals. Resin composites or glass ionomer cements (GICs) are used for the restoration of root surface caries [3]; however, secondary caries is the most common cause of restoration failure [4].

Since GICs were developed in the 1970s, they have been used for restorations of root surface caries due to their performance under wet conditions and fluoride-releasing property. Conventional and resin-modified GICs have unique characteristics, such as anti-cariogenic properties and the ability to adhere directly to teeth structures. Moreover, GICs are capable of releasing fluoride, which acts to enhance tooth tissues via the formation of fluoroapatite, and to remineralize damaged enamel and dentin [5-10]. Although it has been reported that fluoride-release from GICs has the potential to reduce the number of bacteria or interfere with bacterial metabolism in dental plaque [11-14], amounts of fluoride released from GICs are not sufficient and short-lived to

effectively inhibit bacterial growth [15-17]. Therefore, several attempts have been made to provide GICs with antibacterial effects by adding antimicrobial components such as chlorhexidine [18-21], quaternary ammonium compounds [22], silver nanoparticles [23], epigallocatechin-3-gallate [24], or propolis extract [25]. However, the period for these materials to exert antibacterial effects is limited as the release kinetics are not controlled. Moreover, the ecological perturbations *via* the antimicrobial effects displayed by continuous delivery of the agents will exceed thresholds of disrupting homeostasis in an oral environment. Oral microorganisms form a complex ecosystem that thrives in the dynamic oral environment in a symbiotic relationship with the human host [26]. Early (initial) colonizers associated with oral health have substantial ecological advantages. These organisms can bind more avidly to salivary-pellicle-coated teeth, show more rapid growth and antagonize pathogens through multiple mechanisms and helping to maintain microbial homeostasis and stability [26,27]. Nevertheless, once the dental plaque is formed on the surfaces of teeth or materials, the pH values around them are decreased by acids produced from acidogenic bacteria such as *Streptococcus mutans*. Therefore, it is beneficial to provide GICs with an *on-demand* release ability to effectively supply antimicrobial components, when these acidogenic bacteria produce acids in the dental plaque.

BioUnion filler is a glass powder composed of silicon dioxide (SiO₂), zinc oxide (ZnO), calcium oxide (CaO), and fluorine (F) [28]. Particles with silicon-based glass structures can be incorporated into many kinds of dental materials such as tooth surface coatings or restorative materials, and are capable of releasing zinc (Zn²⁺), fluoride (F⁻), and calcium (Ca²⁺) ions. Zn²⁺ is known to contribute to antibacterial effects against oral bacteria and to inhibition of dentin demineralization [29,30]. Ca²⁺ enhances remineralization and inhibits demineralization as well as F⁻ [31]. Therefore, the incorporation of BioUnion fillers would provide various materials with multiple functions via the release of ions. Based on this technology, a GIC for restoration containing BioUnion fillers was developed and commercialized as Caredyne-Restore (GC Corp., Tokyo, Japan) in 2018. As a known antibacterial component, Zn²⁺ inhibits the growth of cariogenic bacteria [32] such as *S. mutans*. Previously, Hasegawa *et al.* reported that a GIC containing BioUnion filler inhibited *S. mutans* biofilm formation by interfering with bacterial adhesion on the surface [33]. Saad *et al.* reported the inhibition of root dentin demineralization and *S. mutans* biofilm formation by a tooth surface coating comprising BioUnion filler [34].

The most unique property of BioUnion filler is its ability to release Zn²⁺ actively in an acidic environment [28]. Therefore, once the dental plaque is formed on the

restoratives incorporating BioUnion filler, the release of Zn^{2+} is expected to be promoted by acids produced by acidogenic bacteria in dental plaque and induce antibacterial effects (Figure 1). However, such *on-demand* Zn^{2+} -release abilities of BioUnion filler or restorative materials containing BioUnion filler and their antibacterial effects against oral bacteria have not yet been elucidated in detail.

OBJECTIVES AND CONTENTS

The purposes of this study were to investigate the release of ions from BioUnion filler and a GIC containing BioUnion filler in an acid environment, and to evaluate their inhibitory effects against the bacteria related to dental plaque formation.

In EXPERIMENT 1, the characterization of BioUnion filler was investigated. Then, its ion release profiles and inhibitory effect against *Streptococcus mutans* were evaluated. Furthermore, Zn^{2+} release from BioUnion filler with repeated exposure to acid and inhibition of *S. mutans* were tested.

In EXPERIMENT 2, the release characteristics of Zn^{2+} from the GIC containing BioUnion filler and its inhibitory effects against oral bacterial species related to dental plaque formation were examined. Then, *in situ* assessments of antibacterial effect of the GIC containing BioUnion filler was conducted.

In EXPERIMENT 3, to assess clinical usefulness of GIC containing BioUnion filler for restorative treatments, physical properties and bonding ability to tooth substrate were investigated.

EXPERIMENT 1

Evaluation of Zn²⁺-release characteristic and antibacterial activity of BioUnion filler

1.1 Materials and Methods

1.1.1 Materials

BioUnion filler (Figure 2; BU) and fluoroaluminosilicate glass powder of a commercial conventional GIC (Fuji VII, GC Corp.; F7 powder) were used. BU was prepared by melting the raw materials of SiO₂, F, CaO, and ZnO in a platinum crucible followed by immediate quenching in distilled water. The prepared glass was ground into particles with a median diameter of 4.5-5.5 μm. The compositions of BU and F7 powder are listed in Table 1.

1.1.2 Characterization of BioUnion filler (BU)

Energy dispersive X-ray spectroscopy (EDS) analysis

The elemental composition of BU was analyzed by field-emission scanning electron

microscope/energy dispersive spectroscopy (FE-SEM/EDS; JSM-F100, JEOL, Tokyo, Japan).

Measurement of solubilities

A total of 0.5 g of each particle was immersed in 100 mL of distilled water (pH 7.0) or acetic acid (pH 4.5). After storage at 37°C for 24 h with shaking at 500 rpm, the particles were filtered through a 0.5 µm filter paper (GC-50, ADVANTEC, Tokyo, Japan), which was weighed beforehand (W_1 g), and dried at 110°C for 1 h. The total weight (W_2 g) of the undissolved particles and the filter paper were then measured, and the solubilities of each particle were calculated according to the following equation:

$$\text{Solubility (\%)} = (0.5 + W_1 - W_2) / 0.5 \times 100$$

The experiments were repeated three times. The data was analyzed using IBM SPSS Statistics 25 (SPSS Inc, Chicago, IL, USA) by analysis of variance (ANOVA) and Tukey's honestly significant difference (HSD) test with a significance level of $p < 0.05$.

X-ray diffraction analysis of BioUnion filler after immersion in water and acids

A total of 200 mg of BU was immersed in 10 mL of water (pH 7.0), acetic acid (pH

4.5), or hydrochloric acid (pH 1.2). After storage at 37°C for 24 h with gyratory shaking at 100 rpm, the particles were dried and mounted on an XRD apparatus (RINT-Ultima2100, Rigaku, Tokyo, Japan). The X-ray beam angle 2θ (degrees) range was set between 10 and 75 degrees and scanned at 0.02 degrees per second. The Cu X-ray source was operated with an acceleration voltage of 40 kV and an electron beam current of 30 mA. Peak positions in the XRD patterns obtained from the specimens were compared and matched with those of the standard material in the powder diffraction file of the International Center for Diffraction Data 2013.

1.1.3 Evaluation of ion release from BU

The profiles of Zn^{2+} , Ca^{2+} , and F^{-} release from BU into distilled water (pH 7.0) or acetic acid (pH 4.5 or pH 5.5) were evaluated. Forty mg of BU were placed in one insert of a transwell with a 0.4 μm filter (96-well Costar Transwell, Corning Inc., Corning, NY, USA). The particles in the insert were immersed in 300 μL of distilled water at pH 7.0 or acetic acid at pH 4.5 or 5.5. After storage at 37°C for 24 h with shaking at 100 rpm, 200 μL of the eluate was collected and the concentration of ions was determined (Figure 3). The eluates were diluted in 4.8 mL distilled water, after which the concentrations of Zn^{2+} and Ca^{2+} were measured using an inductively coupled plasma-optical emission

spectrometer (ICP-OES; iCAP 7000 Series, Thermo Scientific, Cambridge, UK). The concentration of F^- was determined using a fluoride ion electrode (FIE; 6561S-10C, HORIBA, Kyoto, Japan). F7 powder was used for comparison. The experiments were repeated four times. The data was analyzed using IBM SPSS Statistics 25 (SPSS Inc) by ANOVA and Tukey's HSD test with a significance level of $p < 0.05$.

1.1.4 Measurement of MICs and MBCs of Zn^{2+} , Ca^{2+} , and F^- for oral bacteria

Six oral bacterial species (*Streptococcus mutans* NCTC10449, *Streptococcus sobrinus* NCTC12279, *Streptococcus oralis* NCTC11427, *Streptococcus mitis* NCTC12261, *Actinomyces naeslundii* ATCC19246, and *Fusobacterium nucleatum* 1436) were used (Table 2). *S. mutans*, *S. sobrinus*, *S. oralis*, *S. mitis*, and *A. naeslundii* were cultured in a brain-heart infusion (BHI) broth (Becton Dickinson, Sparks, MD, USA) and on BHI agar plates (Becton Dickinson), while *F. nucleatum* was cultured in a Todd Hewitt broth (THB; Becton Dickinson) and on THB agar plates supplemented with 0.1% L-cystein. *S. mutans*, *S. sobrinus*, *S. oralis*, and *S. mitis* were cultured from a stock culture at 37°C for 24 h under anaerobic conditions, while *A. naeslundii* and *F. nucleatum* were incubated at 37°C for 48 h under anaerobic conditions (Table 2).

To evaluate the concentrations of Zn^{2+} , Ca^{2+} , and F^- that can effectively inhibit oral

bacterial growth, measurement of minimum inhibitory concentrations (MICs) and minimum bactericidal concentrations (MBCs) of each ion against 6 bacterial species were measured with a microdilution assay. Briefly, ZnCl₂, CaCl₂ (Wako, Osaka, Japan), and NaF (Sigma-Aldrich, Tokyo, Japan) were dissolved in distilled water to obtain standard solutions of Zn²⁺, Ca²⁺, and F⁻, respectively. Fifty μL of standard solutions with a concentration of 4 – 16384 ppm obtained by serial two-fold dilutions were dropped into the wells of a 96-well microplate. Next, 50 μL of bacterial suspension adjusted to 2.0×10⁶ colony-forming units (CFU)/mL were added to the wells, resulting in the four-fold dilution of the original solution. The microplates were anaerobically incubated at 37°C for 24 or 48 h according to the incubation time for each bacterium shown in Table 2, and the MIC, which is the lowest concentration that prevents visible bacterial growth (turbidity was observed by visual examination), was determined. Then, 100 μL of the sample was taken from the wells that showed no visible growth and inoculated on agar plates. After anaerobic subculturing for 48 h at 37°C, the MBC, which is the lowest concentration of an antibacterial agent required to kill bacterium over a certain period under specific conditions, was determined for the plates that showed no bacterial colonies. The experiments were repeated five times.

1.1.5 Evaluation of antibacterial activity of BU

S. mutans NCTC10449 suspension was adjusted to approximately 1.0×10^4 CFU/mL in BHI broth. A total of 40 mg of BU was placed in a well of a 96-well microplate, and 200 μ L of *S. mutans* suspension (approximately 2.0×10^3 CFU) supplemented with or without 1% sucrose (Wako) was added. After anaerobic incubation at 37°C for 24 h with gyratory shaking at 100 rpm, 100 μ L of the suspension was collected and put into 9.9 mL of BHI broth. The suspension was then serially diluted with BHI broth and inoculated on BHI agar (Becton Dickinson) plates. The plates were incubated anaerobically at 37°C for 24 h, after which the number of colonies formed was determined. F7 powder was used for comparison and bacterial suspension without any particles served as the control. All experiments were repeated three times. The data was analyzed using IBM SPSS Statistics 25 by ANOVA and Tukey's HSD test with a significance level of $p < 0.05$.

1.1.6 Evaluation of Zn²⁺-release from BU with repeated exposure to acid and inhibition of *S. mutans*

A total of 40 mg of BU were placed in one transwell insert, and then immersed in 300 μ L of acetic acid (pH 4.5) at 37°C for 1 day. Next, the particles were immersed in

distilled water (pH 7.0) and stored for 3 days at 37°C while replacing the water every day. This procedure was repeated three times until Day 10 (*i.e.*, the particles were immersed in acetic acid on Days 0–1, 4–5 and 8–9 and in distilled water on Days 1–4, 5–8, and 9–10). The eluates were collected on Days 1–10 and diluted in 5 mL distilled water (Figure 4). The concentrations of Zn²⁺ were measured using ICP-OES. All experiments were repeated five times.

To evaluate the antibacterial effects, the particles of BU were collected on Day 8 (after two times exposure to acetic acid at pH 4.5) using the same methods as described above. The *S. mutans* suspension was adjusted to approximately 1.0×10⁴ CFU/mL in BHI broth with 1% sucrose. The particles were transferred to a well of a 96-well microplate and incubated with 200 µL of *S. mutans* suspension (approximately 2.0×10³ CFU). After anaerobic incubation for 24 h with gyratory shaking at 100 rpm, the viable bacteria were counted (Figure 5). F7 powder was used for comparison and bacterial suspension without any particles served as the control. All experiments were repeated three times. The data was analyzed using IBM SPSS Statistics 25 by ANOVA and Tukey's HSD test with a significance level of $p < 0.05$.

1.2 Results

1.2.1 Characterization of BU

EDS analysis of BU

The elemental composition and elemental mapping images of BU are shown in Table 3 and Figure 6, respectively. The EDS analysis revealed Zn, Ca, F, and Si were detected in BU at a mass fraction of approximately 12.7, 3.0, 5.2, and 9.0% respectively. By the elemental mapping, Si Zn, F, and Ca, were found to be evenly dispersed in the particles.

Measurement of solubilities of BU

Figure 7 shows the solubilities of BU and F7 powder in distilled water or acetic acid (pH 4.5). For both BU and F7 powder, the solubilities into acid were significantly greater than those into distilled water ($p < 0.05$, ANOVA, Tukey's HSD test). Moreover, the solubilities of BU into acid was greater than that of F7 powder.

X-ray diffraction analysis of BU after immersion in water and acids

The XRD patterns of BU after immersion in water, acetic acid, and hydrochloric acid

are shown in Figure 8. Insoluble lanthanum fluoride (LaF_3) was detected on BU after immersion in acetic and hydrochloric acids.

1.2.2 Ion release from BU

The concentrations of Zn^{2+} , Ca^{2+} , and F^- released from BU and F7 powder into distilled water and acetic acid solutions are shown in Table 4. The concentrations of Zn^{2+} and Ca^{2+} released from BU into acetic acid at pH 4.5 were approximately 85 or 73 times higher than those released into the water ($p < 0.05$, ANOVA, Tukey's HSD test). The concentrations of Zn^{2+} and Ca^{2+} released into acetic acid at pH 5.5 were significantly lower than those released into acetic acid at pH 4.5, but higher than those released into the water. Conversely, the concentrations of F^- released into acetic acids from BU at both pH 4.5 and 5.5 were significantly lower than those released into the water.

The release of Zn^{2+} and Ca^{2+} was not found in all eluates of F7 powder, and the concentrations of F^- released from F7 powder into acetic acid solutions at pH 4.5 and 5.5 were significantly lower than those released into the water.

1.2.3 MICs and MBCs of Zn²⁺, Ca²⁺, and F⁻ for oral bacteria

The MICs and MBCs of Zn²⁺, Ca²⁺, and F⁻ against *S. mutans*, *S. sobrinus*, *S. oralis*, *S. mitis*, *A. naeslundii*, and *F. nucleatum* are shown in Table 5. For Zn²⁺, the MIC for the six species ranged from 64 to 128 ppm, whereas the MBC ranged from 512 to 1024 ppm. For Ca²⁺, the MIC for the six species ranged from 256 to 1024 ppm, whereas the MBC ranged from 2048 to 8192 ppm. As for F⁻, the MIC ranged from 128 to 256 ppm, whereas the MBC ranged from 1024 to 8192 ppm. For all bacterial species examined, the MICs and MBCs of Zn²⁺ were smaller than those of Ca²⁺ and F⁻.

1.2.4 Antibacterial activity of BU

Figure 9 shows the number of viable bacteria after incubation in the presence of BU and F7 powder. After 24 h of incubation without the addition of sucrose, colony counts of viable *S. mutans* in the presence of F7 powder were significantly smaller than the control without any particles. The number of surviving cells in the presence of BU (approximately 5.0×10^3 CFU) was significantly smaller compared with F7 powder ($p < 0.05$, ANOVA, Tukey's HSD test). Culture with sucrose significantly enhanced the effects of BU ($p < 0.05$, ANOVA, Tukey's HSD test), and the number of viable cells in the presence of BU (approximately 4.4×10^2 CFU) was smaller than the initial amount

of bacteria (approximately 2.0×10^3 CFU), indicating that BU exhibited a bactericidal effect.

1.2.5 Zn²⁺-release from BU with repeated exposure to acid and inhibition of *S. mutans*

Release profiles of Zn²⁺ from BU with repeated exposure to acetic acid at pH 4.5 are shown in Figure 10A. On Day 1, 505.5 ± 12.6 ppm of Zn²⁺ was released into acetic acid at pH 4.5. The concentrations of Zn²⁺ in water on Days 2–4 decreased dramatically to 29.6 ± 10.1 ppm (mean \pm S.D. for Day 2–4). When the particles were again immersed in acetic acid at pH 4.5, the released amount of Zn²⁺ on Days 5 and 9 increased (418.8 ± 1.8 ppm for Day 5 and 349.8 ± 9.3 ppm for Day 9). Although the concentrations of Zn²⁺ released into both acetic acids on Days 5 and 9 significantly decreased compared with those released on Day 1, the concentrations of Zn²⁺ released from BU increased repeatedly in response to exposure to acetic acids. Additionally, the concentrations released into acetic acids at pH 4.5 were above the MIC value of Zn²⁺ against *S. mutans*.

Figure 10B shows the number of viable *S. mutans* in the presence of BU and F7 powder, which were collected on Day 8 after two times exposure to acetic acid at pH 4.5. Although the number of viable cells in the presence of BU was greater than the

initial amount of bacteria, BU demonstrated significantly greater inhibition of the growth of *S. mutans* compared with F7 powder ($p < 0.05$, ANOVA, Tukey's HSD test).

1.3 Discussion

Hench *et al.* developed a bioactive glass composed of SiO₂, Na₂O, CaO, and P₂O₅ [35,36]. This bioactive glass is a potential candidate for use as filler particles in restorative materials because it can enhance hard tissue regeneration and exert some antimicrobial effects by releasing ions [37,38]. Its antimicrobial effects are attributed to the release of ions such as Ca²⁺, which causes neutralization of the local acidic environment and leads to a local increase in pH that is not well tolerated by bacteria [38-40]. Fluoride-containing bioactive glass that can release and recharge fluoride has been developed to provide cario-static effects [41]. Fluoride at high concentrations is known to exert antibacterial activity against oral bacteria. For instance, the MBC of NaF against *S. mutans* UA159 was reported to be 2500 µg/mL [42]. Such high concentrations of F⁻ are difficult to release from bioactive glasses; therefore, the antimicrobial effects of fluoride-containing bioactive glass are limited. As a result, additional components are needed for GICs to more effectively demonstrate antibacterial effects against oral microorganisms.

BU is a silicon-based glass structure, and zinc, calcium, fluoride and silica were homogeneously distributed inside the particle (Figure 6). The leaching of inorganic ions into water from the fillers varied depending on filler composition and filler treatment [43]. As shown in Figure 7, the solubility of BU into acid is greater than that of F7 powder. This result is possibly related to the incorporation of zinc into the silicate-based glass structure, which increased the solubility of BU in acids compared with F7 powder. Due to the dissolution in acids via an acid-base reaction, Zn^{2+} , Ca^{2+} , and F^{-} in glass can be released under acidic conditions. To evaluate the use of this unique function to promote ion release under acidic conditions, profiles of Zn^{2+} , Ca^{2+} , and F^{-} release from BU into acids were evaluated. F7 powder which is capable of releasing a high concentration of F^{-} [44-46], was used as a control. To determine the pH values of the acids used for release tests, pH changes during incubation of acidogenic *S. mutans* NCTC10449 were confirmed by measuring the pH values of the suspensions. After incubation for 24 h, the pH values of *S. mutans* suspensions with and without sucrose gradually decreased to 4.3 and 5.4, respectively (Figure 11). Based on these results, acetic acid solutions at pH 4.5 and 5.5 were used for release tests. The result of release test indicated that the concentrations of Zn^{2+} and Ca^{2+} released into both acetic acid solutions (pH 4.5 and 5.5) were higher than those released into the water (Table 4).

Zinc or zinc compounds are known to exhibit antibacterial effects against oral bacteria [47]. As described above, a high concentration of fluoride demonstrates antibacterial activity against oral bacteria. To determine the effective concentrations on inhibitory effect of Zn^{2+} , Ca^{2+} , and F^{-} against oral bacteria, the MICs and MBCs for six bacterial species were measured by a microdilution assay. Several studies reported that the MIC/MBC values of zinc against *S. mutans* were smaller than those of fluoride [29,32,48]. Hernández Sierra *et al.* reported a MBC of 500 $\mu\text{g/mL}$ (500 ppm) for Zn against *S. mutans* [49]. Pizzey *et al.* reported that a MIC and a MBC of 2.8 mM (approximately 183 ppm) and 11 mM (approximately 719.38 ppm), respectively, for zinc gluconate against *S. mutans* [51]. They also reported a MIC range of 0.125–0.50 mmol Zn/ml (125–500 ppm) and a MBC range of 1–8 mmol Zn/ml (1000–8000 ppm) for Zn^{2+} against *S. mutans*, *S. sobrinus*, *S. sanguinis*, and *A. naeslundii*. In the present study, the MIC of Zn^{2+} for the examined bacterial species ranged from 64 to 128 ppm, and the MBC ranged from 512 to 1024 ppm; these values are similar to those reported in the previous studies. Moreover, the MICs and MBCs of Zn^{2+} for the examined bacterial species were smaller than those of Ca^{2+} and F^{-} .

Calcium compounds such as calcium hydroxide raise the pH and inhibit oral bacteria when in contact with the aqueous environment [51-53]; however, the

antibacterial activity of Ca^{2+} itself is not strong. This study confirmed that the MICs and MBCs of Ca^{2+} for the examined bacterial species were smaller than those of Zn^{2+} and F^- .

Several studies have reported the inhibitory mechanism of F^- on bacterial metabolic activity [54-56]. Takahashi *et al.* reported that F^- inhibits enolase, which catalyzes the conversion of 2-phosphoglycerate to phosphoenolpyruvate in the Embden-Meyerhof-Parnas pathway in bacterial glycolytic metabolism [57]. Zn^{2+} demonstrates antibacterial activity against gram-positive and gram-negative bacteria [58-62], although the detailed mechanism underlying the antibacterial actions of Zn^{2+} has not been fully elucidated. One study reported that Zn^{2+} can penetrate the cell membranes and disturb the membranes but preserve the integrity of bacterial genome DNA [51]. It has been also reported that Zn^{2+} prevented the synthesis of bacterial cell walls [32,63-65]. Other studies have suggested that zinc acts directly by altering cell proteins via processes such as transmembrane proton translocation, or indirectly by inhibiting protease induced bacterial adhesion [66,67] (Figure 12). Such difference on the antibacterial mechanism between Zn^{2+} and F^- would lead to the result that the MICs and MBCs of Zn^{2+} for the examined bacterial species were smaller than those of F^- .

The result of release test indicated that the concentrations of Zn^{2+} released into

both acids (pH 4.5 and 5.5) were greater than the MIC values against 6 species of oral bacteria (Table 4). Conversely, the concentration of Zn^{2+} released into the water was less than the MICs. The concentrations of Ca^{2+} released into both water and acetic acids were smaller than the MICs of Ca^{2+} against six species. These results indicated that the releases of cationic Zn^{2+} and Ca^{2+} from BU were accelerated under acidic conditions, and that Zn^{2+} released from BU would effectively inhibit the growth of 6 species of oral bacteria. For F^{-} , concentrations released from BU into acetic acid were smaller than those released into the water. XRD analysis indicated that LaF_3 was detected on BU after immersion in acids (Figure 8). It is considered that F^{-} released from BU in acids reacted with La^{3+} included in BU and formed insoluble LaF_3 , thereby lowering the concentration of F^{-} released from BU that was detected in acids.

To evaluate the antibacterial effects of BU and F7 powder, *S. mutans* suspensions with or without added sucrose were incubated in the presence of these powders. The results confirmed that the release of Zn^{2+} from BU more effectively inhibited *S. mutans* than F7 powder. Moreover, BU demonstrated bactericidal effects against *S. mutans* when sucrose was added, whereas growth-inhibitory effects against *S. mutans* growth were observed in the absence of sucrose. As described above, the pH value of *S. mutans* suspensions with added sucrose was smaller after 24 h of incubation than that of

suspensions without added sucrose. Therefore, the inhibition of *S. mutans* by BU was greater for the culture with sucrose than without sucrose, reflecting the decrease in the pH of the suspension in response to the addition of sucrose. The MBC of Zn^{2+} against *S. mutans* NCTC10449 was found to be 512 ppm. While the concentrations of Zn^{2+} released into both acetic acids at pH 4.5 and 5.5 were smaller than the MBC values, higher concentrations of Zn^{2+} were released in response to the incubation of *S. mutans* with sucrose, resulting in bactericidal effects against *S. mutans*. Based on these results, the acidity-induced release of Zn^{2+} from BU exhibited bactericidal or growth-inhibitory effects against *S. mutans*. Once the dental plaque is formed on the surfaces of teeth or materials, the pH values around them are decreased by acids produced from oral bacteria such as *S. mutans* [68-70]. When these acidogenic bacteria produce acids, BU incorporated into materials is capable of releasing Zn^{2+} . In this study, it was confirmed that BU could effectively release Zn^{2+} with repeated exposure to acids, and could inhibit the growth of *S. mutans*. When BU was immersed in acetic acid (pH 4.5), the concentrations of Zn^{2+} increased (Figure 10A). During three times exposure to acetic acid at pH 4.5, the concentrations above the MIC values of Zn^{2+} against *S. mutans* could be maintained. Moreover, the particles after two rounds of exposure to acetic acid (pH 4.5) still inhibited the growth of *S. mutans* in the presence of sucrose (Figure 10B).

However, the concentrations of Zn^{2+} released into the acid gradually decreased after two/three times exposure. It has been reported that ions that act as network modifiers in the structures of bioactive glass such as 45S5 can be released under acidic conditions by the dissolution of the surfaces of particles [71,72]. The release of Zn^{2+} from BU in acids is believed to be accelerated by the dissolution of the particles, but to gradually decrease after repeated exposure to acid with a decreasing surface area of the glass powder. Therefore, the Day 8 samples, which had been exposed to acidic solutions twice, did not exhibit bactericidal effects against *S. mutans* and instead exerted only growth-inhibitory effects. To maintain the bactericidal effects, the ability of Zn^{2+} -release of BU itself should be further enhanced at the level needed to kill *S. mutans* and other oral bacteria by some methods, e.g., recharging with Zn^{2+} solution.

1.4 Summary

BU was capable of releasing Zn^{2+} , Ca^{2+} , and F^- . Under acidic conditions, BU demonstrated accelerated release of Zn^{2+} , which exerted bactericidal or growth-inhibitory effects against *S. mutans* when exposed to acids.

EXPERIMENT 2

Evaluation of Zn²⁺-release characteristic and antibacterial activity of a GIC containing BioUnion filler

2.1 Materials and Methods

2.1.1 Materials

Table 6 shows the materials used. For GIC containing BU, Caredyne Restore (GC Corp.; CA) was employed. The powder and liquid of CA were mixed in a ratio of 2.3 : 1 (w/w) and the paste was poured into a mold (9 mm diameter, 2 mm thickness), pressed with a celluloid strip and glass slide, and stored at 25°C for 24 h. The specimen was then polished using silicon carbide grinding papers (#120 to #2500; Buehler, Lake Bluff, USA). A conventional GIC (Fuji VII, GC Corp.; F7) and a resin composite (MI FIL, GC Corp.; MI) were used for comparison. The powder and liquid of F7 were mixed in a ratio of 1.8 : 1 (w/w), and the set cement was prepared by the same method as described above. To prepare a cured specimen of MI, the paste was poured into a mold (9 mm diameter, 2 mm thickness), covered with celluloid strips and a glass slide, and cured for 40 s using a light activation unit (Quick Light VL-1, Morita, Kyoto, Japan).

Finally, the specimens were polished as described above. Before testing, the surface of specimens was disinfected with 70 vol% ethanol.

2.1.2 Evaluation of ion release from the GIC containing BU (CA)

The release of Zn^{2+} , Ca^{2+} , and F^{-} from CA into the water and acetic acid were evaluated.

The set specimens were immersed in 300 μ L of distilled water at pH 7.0 or acetic acid at pH 4.5 in a 48-well microplate (Tissue Culture Plate; VIOLAMO, Osaka, Japan) at 37°C for 24 h and shaken at 100 rpm. Then, 200 μ L of the eluate was collected and the concentration of ions was determined. The eluates were diluted with 4.8 mL of distilled water, and the concentrations of Zn^{2+} and Ca^{2+} were measured by ICP-OES. The concentration of F^{-} was determined using the fluoride ion electrode. The experiments were repeated four times.

To evaluate the release of Zn^{2+} from CA with repeated exposure to acetic acid, the set specimens were immersed in 300 μ L of acetic acid (pH 4.5) in a 48-well microplate at 37°C for 1 day and then immersed in distilled water (pH 7.0) at 37°C for 3 days with the water replaced every day. The procedure was repeated seven times for a total of 28 days. That is, the specimens were immersed in acetic acid on Days 1, 5, 9, 13, 17, 21, and 25, and in distilled water on the other days (Figure 13). A total of 200 μ L eluate

was collected every day, diluted with 4.8 mL of distilled water, and the concentration of Zn^{2+} was measured by ICP-OES. All the experiments were repeated five times. The statistical data was analyzed using IBM SPSS Statistics 25 by ANOVA and Tukey's HSD test with a significance level of $p < 0.05$.

2.1.3 Elemental analysis of CA

The elemental analysis of set CA was carried out by FE-SEM/EDS. To evaluate the influence of repeated exposure to acid on the distribution of each element, the specimens were immersed in acetic acid and distilled water for 28 days (after exposure to acetic acid seven times) by the same protocol with ion release test in 2.1.2, and the specimens collected on Day 28 were analyzed by FE-SEM/EDS.

2.1.4 Evaluation of antibacterial activity of CA

Human unstimulated saliva was collected from four healthy donors, which was approved by the Ethics Review Committee of Osaka University Graduate School of Dentistry and Osaka University Dental Hospital (Approval number: R1-E52). The collected saliva was filtered twice with a 0.22 μm syringe filter, and the set specimens of CA were immersed in 1 mL of filtered saliva for 2 h at 37°C.

Six species of bacteria (Table 2) were cultured in broth and adjusted to approximately 1.0×10^6 CFU/mL. To evaluate the growth of each bacterial species in contact with the surface of the set CA after treatment with human saliva, an on-disc culture assay was performed. Twenty μL of bacterial suspension (2.0×10^4 CFU) supplemented with 1% sucrose was inoculated on the disc and anaerobically incubated at 37°C for 24 or 48 h. The inoculated discs were then transferred to 9.98 mL of respective broths and vigorously shaken for 10 s to collect bacteria from the surface. The suspension was serially diluted, and aliquots of the suspension were spread on agar plates. After anaerobic incubation at 37°C for 24 or 48 h, the number of colonies was counted. The experiment was repeated five times. F7 and MI were used for comparison.

To evaluate the antibacterial effects after repeated exposure to acetic acid, the specimens were immersed in acetic acid (pH 4.5) and distilled water by the same protocol as that used for the ion release test in 2.1.2. On Day 4, 8, and 24 (exposure of the specimens to acetic acid for one, two, and six times, respectively), the specimens were immersed in 1 mL of filtered saliva for 2 h at 37°C . The suspensions of the six bacterial species were adjusted to approximately 1.0×10^6 CFU/mL with respective broth (Table 2) supplemented with 1% sucrose, and the antibacterial effects were evaluated by an on-disc culture assay (Figure 14). Each bacterial suspension with 1%

sucrose (20 μ L) was inoculated on each disc, which was collected on Day 4, 8 or 24 and treated with filtered saliva. After anaerobic incubation at 37°C for 24 or 48 h, the viable bacteria were counted as described above. All the experiments were repeated five times. F7 and MI were used for comparison.

2.1.5 Evaluation of bacterial adherence to CA

The disc-shaped set specimen was immersed in 1 mL of filtered saliva for 2 h at 37°C and fixed with a steel wire so that the disc was positioned in the center of a tube (29×75 mm, AGC Techno Glass Co., Ltd., Shizuoka, Japan). Each bacterium of six species was cultured in respective broth (Table 2) and adjusted to approximately 1.0×10^6 CFU/mL, and 20 mL of bacterial suspension supplemented with 1% sucrose was added into the tube. After anaerobic incubation at 37°C for 24 or 48 h with shaking at 100 rpm, the specimen was retrieved from the suspension and rinsed three times with 20 mL of phosphate buffered saline (PBS; Wako). The bacteria attached to the surface of the specimen were scraped using a microbrush, which was then transferred to 10 mL of broth and sonicated for 10 min in an ultrasonic bath at 37 kHz and 300 W to detach the bacteria. The number of bacteria in the broth was calculated by plating them on agar plates and anaerobically incubating them for 48 h. F7 and MI were used for comparison.

2.1.6 *In situ* assessments of antibacterial effect of CA

Study subjects

The study of *in situ* evaluation included healthy 3 subjects (2 men and 1 woman) aged 29-38 years (mean 32.3±4.0 years) who were the students and staff of the Osaka University Graduate School of Dentistry. No clinical signs of caries, gingivitis, or periodontitis were detected, and no systemic disease was observed in any of the subjects. The subjects abstained from antibiotics 6 months before the study commenced. Written informed consent was obtained from all subjects. The study design was reviewed and approved by the Ethics Committee of the Osaka University Graduate School of Dentistry and Osaka University Dental Hospital (Approval number: R2-E19). The experiments were performed in accordance with ethics guidelines concerning medical science studies of humans.

In situ biofilm formation

Three subjects wore a custom-made acrylic splint in their upper jaw for 24 h to form oral biofilms. In the splint, eight disc-shaped specimens including CA, F7, and MI were fixed with an ethylcyanoacrylate-based glue (Aron Alpha, Toagosei Co., Ltd., Tokyo, Japan) in the region of upper premolars and molars of each subject (Figure 15). The

subjects wore the splint for 24 h, except during meals (15 min \times 3 = 45 min) and while brushing their teeth (15 min \times 2 = 30 min). During each meal, the appliance was immersed in 6% sucrose solution. After the wearing, the specimens were collected from the splint without disrupting the adherent biofilm. Subsequently, the specimens were gently irrigated twice with 1 mL of PBS.

Observation of biofilms using a confocal laser scanning microscopy

Biofilms formed on the samples were stained using LIVE/DEAD[®] BacLight[™] bacterial viability kits (L7007, Molecular Probes, Eugene, OR, USA) according to the manufacturer's instructions. Briefly, 2 μ L of component A (SYTO 9 dye, 1.67 mM/propidium iodide, 1.67 mM solution in DMSO) and 2 μ L of component B (SYTO 9 dye, 1.67 mM/propidium iodide, 18.3 mM solution in DMSO) were mixed in 1 mL of distilled water. 100 μ L of the mixed solution was dropped on the specimen and incubated at 37°C for 15 min under dark condition. After gently irrigating with distilled water, the specimen was visualized using a confocal laser scanning microscope (CLSM; LSM 700, Carl Zeiss, Oberkochen, Germany) at 488 and 555 nm for excitation, and 500 and 635 nm for emission.

The images were obtained using a ZEN Imaging Software (Carl Zeiss,

Oberkochen, Germany). A preliminary image was taken to determine the acquisition parameters and the setting was kept constantly for all images. Scans were taken in 12 bits at a resolution of 1024 by 1024 with the following setting: Speed = 8; Pinhole size = 34 μm ; Digital offset = 0; Master gain (Ch1, SYTO 9) = 493; Master gain (Ch2, propidium iodide) = 706. Three images were obtained from one sample, and the images were analyzed by Imaris software (Bitplane, Zurich, Switzerland) to determine the thickness of biofilm.

Quantification of bacterial cells in biofilms

Biofilms adhered to the surface of specimen was scraped using a micro brush. Then, the micro brush was transferred to 10 mL of PBS and sonicated to detach bacteria for 10 min in an ultrasonic bath operating at 37 kHz and 300 W. The suspension was serially diluted and aliquot of suspension was spread on Trypticase Soy Agar with 5% sheep blood (Nippon Becton Dickinson, Tokyo, Japan). After anaerobic incubation at 37°C for 24 h, the number of colonies was counted.

2.2 Results

2.2.1 Ion release from CA

The concentrations of Zn^{2+} , Ca^{2+} , and F^- released from CA and F7 into distilled water and acetic acid solutions within 24 h are shown in Table 7. The concentration of Zn^{2+} released from CA into acetic acid at pH 4.5 was significantly higher than that into the water. In contrast, the concentration of F^- released into acetic acid was significantly lower than that into the water ($p < 0.05$ ANOVA, Tukey's HSD test). The release of Zn^{2+} and Ca^{2+} was not found from F7, and the concentration of F^- released from F7 into the water was significantly higher than that into acetic acid ($p < 0.05$ ANOVA, Tukey's HSD test).

The release profiles of Zn^{2+} for CA over 28 days are shown in Figure 16. The concentration of Zn^{2+} released into acetic acid at pH 4.5 on Day 1 (170.4 ± 7.0 ppm) was significantly higher than that into the water. The release of Zn^{2+} about 170 ppm was obtained at every exposure to acetic acid, and no significant decrease in the concentration of Zn^{2+} released from CA into acid was found ($p > 0.05$, ANOVA, Tukey's HSD test).

2.2.2 Elemental analysis of CA

Table 8 shows elemental compositions of CA. Figure 17 shows the FE-SEM image and EDS elemental mapping images of CA. Si and F are distributed around the glass particles, whereas Zn and Ca are homogeneously distributed in both the particles and the matrix. No differences were observed in the distributions of Zn and Ca before and after exposure to acetic acid for 28 days.

2.2.3 Antibacterial activity of CA

Figure 18 shows the number of viable bacteria after incubation on CA, F7, or MI before and after repeated exposure to acid. Compared with F7 and MI, a significantly smaller number of bacterial colonies ($p < 0.05$, ANOVA, Tukey's HSD test) were obtained for all species by culturing on CA before exposure to acid (Day 0). Moreover, the numbers of viable cells of the examined bacterial species on CA were the same or smaller than the initial amounts of bacteria (2.0×10^3 CFU).

Significantly greater inhibition of the growth of all bacterial species compared with F7 and MI was observed for CA on Day 4, 8, and 24 ($p < 0.05$, ANOVA, Tukey's HSD test), indicating that the antibacterial effect of CA against the six bacterial species was maintained even after repeated exposure to acetic acid.

2.2.4 Bacterial adherence to CA

Figure 19 shows the number of bacteria adhered to CA, F7, and MI. CA significantly inhibited the adherence of the examined bacterial species, as compared with F7 and MI ($p < 0.05$, ANOVA, Tukey's HSD test).

2.2.5 *In situ* assessments of antibacterial effect of CA

Representative CLSM images (Figure 20A) revealed that the biofilm formed on CA was sparser and thinner than those on F7 and MI. Figure 20B shows the analysis of CLSM images. Biofilms formed on CA was significantly thinner than F7 and MI ($p < 0.05$, ANOVA, Tukey's HSD test).

The number of surviving cells in the biofilm formed on CA was significantly smaller than that of F7 and MI as shown in Figure 20C ($p < 0.05$, ANOVA, Tukey's HSD test).

2.3 Discussion

BioUnion filler (BU) has a silicon-based glass structure and is capable of releasing Zn^{2+} , Ca^{2+} , and F^- . In EXPERIMENT 1, it was shown that acidic conditions promoted the release of Zn^{2+} from BU itself owing to the acid-solubility. To confirm such

characteristic of BU when incorporated in a GIC, the release of Zn^{2+} , Ca^{2+} , and F^{-} from CA was evaluated. For Zn^{2+} , it was found that the concentration (170.4 ± 7.0 ppm) released into acetic acid was higher than the MIC range (64–128 ppm) against the examined oral bacterial species, whereas the concentration released into the water was lower than this range. For Ca^{2+} and F^{-} , the concentrations of both ions released into acetic acid were lower than the respective MICs. GICs are formed by an acid-base reaction between a basic fluoroaluminosilicate glass and polyacrylic acid [73]. The aluminosilicate glass contains Ca^{2+} , Al^{3+} , and Si^{4+} , which are linked to each other by bridging oxygens. When aluminosilicate glass and polyacrylic acid are mixed, the protons of polyacrylic acid degrade the surface of aluminosilicate glass, and the bonds in the glass network are hydrolyzed; consequently, Ca^{2+} and Al^{3+} are liberated. The Ca^{2+} and Al^{3+} subsequently bind with the carboxyl groups, thereby forming the matrix. A silica gel layer is formed around the remaining glass particles, which impedes further degradation [74-77]. Ca^{2+} and Al^{3+} in the matrix can be released into acids via ion exchange between H^{+} and Ca^{2+}/Al^{3+} [78,79]. In the case of CA, Zn^{2+} and Ca^{2+} are liberated from BU upon mixing the powder with polyacrylic acid. The EDS analysis showed homogeneous distribution of Zn and Ca in both the particles and the matrix, indicating that Zn^{2+} and Ca^{2+} liberated from BU were bound to the polyalkenoate

groups or trapped in the matrix of CA (Figure 21). The results of ion-release tests indicate that Zn^{2+} in the matrix and residual glass core of CA can be effectively released when the set GIC is exposed to acid. The findings of EDS analysis that distribution of Zn was not affected after repeated exposure to acetic acid supports such mechanism of Zn^{2+} -release from CA.

The release of Zn^{2+} from CA with repeated exposure to acid was confirmed by repeatedly immersing the specimen in acetic acid for 1 day and in distilled water for 3 days. During 28 days with seven times repeated exposure to acetic acid, release of Zn^{2+} at an effective concentration higher than the MIC for the six bacterial species was maintained. The amount of zinc (W_z mg) incorporated in the CA disc (9 mm diameter, 2 mm thickness) was assumed to be approximately 14.5 mg, which was calculated by the weight of disc (W_d mg) and mass% of Zn in the cement ($M_z\%$) determined by EDS analysis; $W_z = W_d \times M_z \times 1/100$. The total amount of Zn released from CA during seven times exposure to acid for 28 days was approximately 1.2 mg; thereby, the percentage of the release amount of Zn from CA was only 8.3%. If all Zn incorporated in CA was released, CA would be capable of releasing Zn with 84 times exposure to acid for 337 days. In this experiment, the CA disc was immersed in pH4.5 of acetic acid for 24 h to evaluate the release behavior of Zn^{2+} during repeated exposure to acid. However,

Stephan [80] and other studies [81,82] have reported that pH value of plaque reduced up to pH4.5-6 and gradually returned during 60 min after sucrose uptake. Although it is not possible to precisely speculate the duration of Zn²⁺-release in the clinical settings from the results of this study, long-lasting *on-demand* release of Zn²⁺ from CA can be expected.

Oral biofilms are composed of a complex mixture of different bacterial species and are formed by a highly ordered sequence of events, starting with the attachment of initial colonizing bacteria (streptococci, etc.) to the tooth surface with the acquired pellicle followed by the coaggregation of late colonizers [83]. During biofilm formation, *F. nucleatum* acts as a bridging organism connecting the early and late colonizing bacteria [84]. *S. mutans* and *S. sobrinus* along with a group of bacteria initiate dental caries by producing extracellular glucans from sucrose as well as acid [85], whereas *A. naeslundii* is the pathogen of root surface caries [86,87]. Therefore, an on-disc culture assay was conducted to examine the antibacterial activities of CA, F7, and MI using six species of bacteria. When the 10 mL suspension of *S. mutans* NCTC10449, *S. sobrinus* NCTC12279, *S. oralis* NCTC11427, or *S. mitis* NCTC12261 in the broth adjusted to approximately 1.0×10^6 CFU/mL were grown, the numbers of bacteria after 24-h incubation reached up to $(7.3 \pm 1.6) \times 10^8$, $(5.7 \pm 2.2) \times 10^8$, $(4.9 \pm 1.1) \times 10^8$, and

$(6.7\pm 1.3)\times 10^8$ CFU/mL, respectively. The growth of anaerobic *A. naeslundii* and *F. nucleatum* was comparably slow, and it took 48 h to reach up to $(3.4\pm 1.2)\times 10^8$ and $(2.7\pm 0.8)\times 10^8$ CFU/mL. In our on-disc culture assay, 20 μ L bacterial suspension at 1.0×10^6 CFU/mL was cultured, but the number of six species of bacteria was increased to 4.3 - 6.9 \log_{10} CFU by 24 or 48-h incubation on the control material MI. Those are similar with the bacterial number after incubation of each bacterium in 10 mL broth described above. Therefore, on-disc culture assay utilized in this study can be validated as the method with enough nutrient condition for all of six bacteria to grow.

The results of on-disc culture assay demonstrated that CA inhibited the growth of all the examined bacterial species more effectively than F7, indicating the effectiveness of Zn^{2+} released from CA. In this test, the bacterial suspensions containing sucrose was incubated on the set cement. The pH changes during the incubation of bacteria (in the absence of any materials) were confirmed by measuring the pH of the suspensions with 1% sucrose. After incubation for 24/48 h, the pH of the *S. mutans*, *S. sobrinus*, *S. oralis*, *S. mitis*, *A. naeslundii*, and *F. nucleatum* suspensions gradually decreased to 4.3 (24 h), 4.2 (24 h), 4.5 (24 h), 4.4 (24 h), 4.6 (48 h), and 4.7 (48 h), respectively. Further, the pH changes during incubation was monitored, which revealed that the inhibitory effects of CA against the growth of the examined bacterial species were due to the release of

Zn²⁺ from CA induced by the acids produced by these bacteria. Moreover, the numbers of viable cells of *S. mutans*, *S. sobrinus*, *S. oralis*, *S. mitis*, *A. naeslundii*, and *F. nucleatum* on CA after incubation decreased, while the concentration of Zn²⁺ released into acetic acid during the release test was lower than the MBC range of Zn²⁺ for the six bacterial species. It is considered that the concentration of Zn²⁺ released into the bacterial suspensions was higher than that released into acetic acid since the volume of suspensions (20 µL) used for on-disc culture assay was 15 times smaller than that of acetic acid (300 µL) used in 2.1.2. Considering that the concentration of Zn²⁺ release from CA was maintained across seven times exposure to acid (Figure 16), the acidity-induced release of Zn²⁺ was responsible for strong inhibitory effects observed repeatedly (Figure 18).

Ion-releasing inorganic fillers have been intensively studied for application in restorative and preventive treatments with antibacterial activity. The eluate from the ion-releasing materials suppresses the adherence of oral bacteria, thereby inhibiting oral biofilm formation on the surface of restorative materials [28]. In this study, bacterial attachment on CA after incubation of the specimen in bacterial suspensions was significantly less than that on F7 and MI (Figure 19). This suggests that the Zn²⁺-releasing ability of CA resulted in the inhibition of not only bacterial growth, but also

bacterial adhesion, leading to the inhibition of oral biofilm formation. Interestingly, no adherent cells of *F. nucleatum* were observed on CA. *F. nucleatum* basically may have weak adherence capacity directly to restorative materials as this bacterium mainly serve as a “bridging organism” between early and late colonizers in dental plaque [84,88]. However, as shown in Figure 18F, CA can inhibit the growth of *F. nucleatum* on its surface. Such inhibition of the “bridging organism” by the release of Zn^{2+} is considered to be effective to inhibit formation of dental plaque.

To evaluate the antibacterial effect of CA in an oral cavity, *in situ* assessment was conducted using a modification of a previously reported *in situ* biofilm model [89, 90]. The results indicated that CA reduced the thickness of biofilm formed on its surface and the number of bacteria in the biofilm. During three meals for total 45 min, the specimens fixed on the acrylic splint were immersed in 6% sucrose solution, which would promote the acid production from bacteria (streptococci or lactobacilli, etc.) and decrease pH of biofilm formed on specimens. This condition might be preferable for CA that can release Zn^{2+} under acidic conditions and lead to the inhibition of bacterial growth/attachment in biofilms. Furthermore, the reduction in number of acidogenic bacteria such as *S. mutans* can reduce acid production which is the main virulence factor leading to tooth demineralization [91,92]. Although, in this study, the effect of CA on

the prevention of caries formation was not directly investigated, reduction in the number of cariogenic bacteria and inhibition of oral biofilm formation on the material are supposed to contribute to prevention of recurrent caries on root surface. It has been reported that the concentration of H^+ production was related to the number of viable cariogenic cells of the biofilm [93]. In this study, the thinner biofilm was formed on CA, related to lower viable bacterial number including cariogenic bacteria adhered. Thus, antibacterial effects exhibited by CA reduce the virulence of the biofilm, and help prevent demineralization of the tooth adjacent to restorations. The root cementum has high organic content and has a highly cross-linked collagen structure, and is less hard compared with enamel and dentin. Such characteristics make cementum more vulnerable to acid attack, and the critical pH for cementum to be demineralized was reported to be pH 6.2-6.7 [94-96]. Thus, a slight pH decrease in the dental plaque leads to demineralization of the root tissues and the development of root surface caries. Therefore, further investigations such as measurements of pH reduction in *in situ* biofilm formed on CA and release amounts of Zn^{2+} from CA into its biofilm are required to assess the effectiveness of CA on prevention of root surface caries. However, it is difficult to monitor the pH change in *in situ* biofilm and evaluate the concentration of Zn^{2+} released from CA in biofilm formed on its material. To address such limitation of

in situ assessments and assess the clinical efficacy of CA on antibacterial/anti-biofilm properties, an *in vitro* culture system that reproduces *in situ* oral biofilm formed on restorative materials may be useful. Moreover, it has been reported that CA also demonstrated inhibitory effects of tooth demineralization and enhancement of remineralization due to the release of Zn^{2+} [97-99]. The evaluation of such characteristics of CA using the *in vitro* model that mimic oral environment would help assess the efficacy of CA on prevention of root surface caries.

Oral microbiota consists of diverse microorganisms that produce complex and harsh oral biofilm. It has been reported that several species, such as *S. salivarius*, is a primary source of urease in the oral cavity [100]. *S. salivarius* is an abundant isolate of the human oral microbiota. Since urea is the most abundant nitrogen source in the saliva and crevicular fluids [101], the presence of ureolytic *S. salivarius* is critical for maintaining the pH of the oral ecosystem and preventing the development of dental caries [102]. Therefore, further investigation is required to investigate the influence of Zn^{2+} released from CA on these bacteria or bacterial composition in oral biofilms.

2.4 Summary

The release of Zn^{2+} from CA was accelerated under acidic conditions, and the growth

of six oral bacteria was effectively inhibited on CA when exposed to acid environment repeatedly. CA also demonstrated inhibition of the adherence of the six bacterial species. Furthermore, *in situ* assessment revealed that CA could inhibit early-stage biofilm formation on its surface.

EXPERIMENT 3

Evaluation of physical properties and bonding ability of CA

3.1 Materials and Methods

3.1.1 Setting time

The setting time of CA was measured according to International Organization for Standardization (ISO) 9917-1:2007 [103]. The powder and liquid of CA were mixed, and the paste was placed in a stainless-steel mold (10 mm length, 8 mm width, 5 mm high). The entire assembly was then transferred to an incubator (37°C, >90% relative humidity). A Vicat needle with a weight of 400 g and an active tip of 1.0 mm diameter was used. The needle was lowered vertically onto the horizontal surface of the cement, and the setting time was taken as the point at which the indenter needle failed to make an indentation. The time from the start of mixing until the setting of the cement was recorded as the setting time. F7 was used as a control. Five specimens (n = 5) were prepared for each material and used for the measurement.

3.1.2 Acid erosion

The acid erosion of CA was tested according to ISO 9917-1:2007 [103]. A poly(methyl methacrylate) (PMMA) disc (30 mm diameter, 5 mm thickness) with a hole (5 mm diameter, 2 mm depth) in the center was prepared. The hole in the PMMA disc was filled with CA, covered with a polyester sheet, pressed firmly, and clamped. At 180 s after the end of cement mixing, the entire assembly was transferred to an incubator (37°C, >90% relative humidity). After 24 h, the clamp and polyester sheet were removed, and the specimen was polished with 1200 grit abrasive paper until a flat surface was obtained. The initial depth at the center of the specimen was measured at five points with the edge of the specimen holder taken as a fixed reference plane. The height at the center of the specimen was subtracted from the average height of the specimen holder to obtain an initial height of the cement (D_0). The specimen was placed horizontally in a bottle containing 30 mL of an erosion solution composed of 0.1 mol/L lactic acid/sodium lactate buffer solution adjusted to pH 2.74 ± 0.02 . After 24 h of immersion at 37°C, the specimen was removed and rinsed with distilled water. Subsequently, the height of the center was measured again (D_t). The eroded depth, D (in mm), at the center of each specimen was calculated by the equation $D = D_0 - D_t$. F7 was used for comparison. Five specimens ($n = 5$) were prepared for each material and

used for the measurement.

3.1.3 Compressive strength

Compressive strength before exposure to acid

The compressive strength of CA was evaluated according to ISO 9917-1:2007 [103].

The powder and liquid of the cement were mixed and packed slightly excessively in a stainless-steel mold with internal dimensions of 4 mm (diameter)×6 mm (height). After setting for 1 h, the specimen was removed from the mold and immersed in distilled water at 37°C for 24 h. The specimen was then dried, and a compressive load was applied along the long axis of the specimen at a crosshead speed of 0.75±0.30 mm/min using a universal testing machine (Autograph AG-1kNIS, Shimadzu, Kyoto, Japan).

The compressive strength (Σ) of the upright cylindrical sample with the area (A) was calculated according to the following formula:

$$\Sigma = F/A$$

where: F = maximum load applied to the specimen (N), A = area (m²). F7 was used for comparison. Five specimens (n = 5) were prepared for each material and used for the measurement.

Compressive strength after repeated exposure to acid

To evaluate the effect of repeated exposure to acetic acid on the compressive strength of CA, the specimens were repeatedly immersed in acetic acid at pH 4.5 and distilled water by the same method as that described for the ion release test in 2.1.2. Using the specimen on Day 28 (after exposure to acetic acid for seven times), the compressive strengths was measured as mentioned above. F7 was used for comparison. Five specimens ($n = 5$) were prepared for each material and used for the measurement.

3.1.4 Toothbrush wear

The flat specimen (7.3 mm diameter, 1.5 mm thickness) of CA was prepared and polished using silicon carbide paper from 240 to 4000 grit. Using a wear tester (Tokyo Giken, Tokyo, Japan), a toothbrush (Prospec, GC Corp.) with dentifrice (white & white, Lion Dental Products, Tokyo, Japan) hit flat specimens 120000 times with a 200 g weight and a lateral movement of 30 mm. The thickness of the specimen was measured using a caliper (Mitutoyo, Tokyo, Japan) and the vertical loss was calculated as the amount of toothbrush wear. F7 was used for comparison. Four specimens ($n = 4$) were prepared for each material and used for the measurement.

3.1.5 Bond strength to enamel and dentin

Crown of bovine incisors was embedded in an acrylic resin (UNIFAST II, GC Corp.,) with the buccal surface facing upward. The surface was planarized with 120 grit silicon carbide paper to expose the flat enamel or dentin, and polished with 320 grit silicon carbide paper. A cylindrical polyethylene mold with internal dimensions of 2.4 mm (diameter)×3 mm (height) (Ultradent Inc, South Jordan, UT, USA) was set on the exposed enamel/dentin. Subsequently, the powder and liquid of CA were mixed, and the resulting paste was poured into the mold. The specimens were stored at 37°C in a relative humidity of >90% for 5 min, and then removed from the cylindrical mold and stored in distilled water at 37°C for 24 h. The shear bond strength test was conducted using a tabletop testing machine (EZ-S, Shimadzu) at a crosshead speed of 1.0 mm/min. The shear bond strength was calculated by dividing the load by the bonded area (4.52 mm²). F7 was used as a control. Six specimens (n = 6) were prepared for each material and used for the measurement.

3.2 Results

3.2.1 Setting time

Table 9 lists the physical properties of CA and F7. The setting time of CA was 165 s which fulfilled the requirement described in the ISO 9917-1 [103].

3.2.2 Acid erosion

The acid erosion of CA was significantly less compared with F7 ($p < 0.05$, ANOVA, Tukey's HSD test), and fulfilled the requirement described in the ISO 9917-1 [103].

3.2.3 Compressive strength

The compressive strength of CA before exposure to acid was 146.8 ± 5.2 MPa (Table 9) which showed no significant difference from F7 ($p > 0.05$, ANOVA, Tukey's HSD test), and fulfilled the requirement described in the ISO 9917-1 [103].

For both CA and F7, no significant differences were observed in the compressive strengths before and after exposure to acid ($p > 0.05$, ANOVA, Tukey's HSD test). Even after being exposed to acetic acid seven times, the compressive strength of CA fulfilled the requirement described in the ISO 9917-1 [103].

3.2.4 Toothbrush wear

The toothbrush wear of CA was 6.4 ± 5.4 μm (Table 9), and no significant differences

were observed between CA and F7 ($p > 0.05$, ANOVA, Tukey's HSD test).

3.2.5 Bond strength to enamel and dentin

The shear bond strengths to enamel and dentin of CA and F7 are shown in Table 9. For both enamel and dentin, there were no significant differences between CA and F7 ($p > 0.05$, ANOVA, Tukey's HSD test).

3.3 Discussion

The particle size and composition of glass fillers affect the physical properties of GICs [104]. BioUnion filler has a particle size of approximately 4.5-5.5 μm , which is within the range of the particle size of commercial GICs [105]. The setting time, compressive strength, and acid erosion of CA fulfilled the requirement described in the ISO 9917-1. In addition, all physical properties measured and shear bond strengths of CA were equivalent to those of conventional GIC (F7). Moreover, the toothbrush wear of CA was also equivalent to F7. These results reveal that CA demonstrated acceptable physical properties for clinical use.

To assess if the release of Zn^{2+} would jeopardize the longevity of restoration using CA, compressive strength after repeated exposure to acetic acid was measured.

The results demonstrated no reduction in compressive strength, which implies that the release of Zn^{2+} from the matrix of CA does not deteriorate its physical properties. The acidity-induced release of Zn^{2+} from CA is considered to occur through ion exchange between H^+ and Zn^{2+} . In addition, it has been reported that the ionomer reaction of GICs persists for a long time (known as *maturation*) and improves their mechanical properties due to the maturation of cements [106]. Likewise, in combination with possible long-term ionomer reaction, the compressive strength of CA was maintained even after being exposed to acetic acid seven times.

It is well known that GICs show bonding ability to tooth structure based on chelation reaction of polycarboxylate group with Ca of hydroxyapatites [107]. For both to enamel and dentin, shear bond strength of CA was not significantly different from that of F7. CA is a kind of GIC, which set by the acid-base reaction of the glass and polyacrylic acid, and therefore useful for the restoration where the moisture control is difficult. Considering its additional property to exert antibacterial effects, the fact that CA shows the bonding ability equivalent to conventional GIC indicates advantage for root surface restorations.

3.4 Summary

CA demonstrated acceptable physical properties and bonding ability for clinical use.

Also, it was confirmed that Zn^{2+} -release from BU in an acidic environment does not affect the compressive strength of CA.

GENERAL CONCLUSIONS

Glass ionomer cements (GICs) have been widely used for restorations of root surface caries due to their performance under wet conditions and fluoride-releasing property.

As the GICs cannot effectively inhibit the bacterial growth and biofilm formation, further modification to provide the ability to prevent recurrent caries is needed. With the objective of improving the antibacterial effects of GICs, a new GIC that employed BioUnion filler was developed.

This study confirmed that BioUnion filler, a new bio-active glass powder could demonstrate accelerated release of Zn^{2+} , which exerted bactericidal or growth-inhibitory effects against oral bacterial. The release of Zn^{2+} from GIC incorporating BioUnion filler was also accelerated under acidic condition, demonstrating effective inhibition of oral bacterial growth and adherence. Such acidity-induced ability to release Zn^{2+} of GIC containing BioUnion filler is able to hinder early-stage biofilm formation, which is expected to be of benefit in the prevention of recurrent caries on the root surface.

This unique function of BioUnion filler would be beneficial to be combined in

other dental materials such as resin composites, CAD/CAM blocks, luting or orthodontic cements. However, the possibility of combination with resin-based materials have to be further elucidated.

Once the GIC containing BioUnion filler, releases Zn^{2+} and inhibits the acidogenic bacteria, pH in biofilms increases; thereafter, the material would not release further ions.

Such *on-demand* release of antibacterial components may lead to the maintenance of homeostasis in an oral environment and have less adverse influence on oral ecosystem.

Therefore, an assessment of the benefit of this material is still required to examine its potential for maintenance of microbial composition in the oral environment.

REFERENCES

- [1] van Houte J. Role of micro-organisms in caries etiology. J Dent Res 1994; 73: 672-681.
- [2] Imazato S. Bio-active restorative materials with antibacterial effects: new dimension of innovation in restorative dentistry. Dent Mater J 2009; 28: 11-19.
- [3] Yengopal V, Mickenautsch S. Caries-preventive effect of resin-modified glass-ionomer cement (RM-GIC) versus composite resin: a quantitative systematic review. Eur Arch Paediatr Dent 2011; 12: 5-14.
- [4] Gluzman R, Katz RV, Frey BJ, McGowan R. Prevention of root caries: a literature review of primary and secondary preventive agents. Spec Care Dentist 2013; 33: 133-140.
- [5] Mitra SB. *In vitro* fluoride release from a light-cured glass-ionomer liner/base. J Dent Res 1991; 70: 75-78.
- [6] Seppä L, Korhonen A, Nuutinen A. Inhibitory effect on *S. mutans* by fluoride-treated conventional and resin-reinforced glass ionomer cements. Eur J Oral Sci 1995; 103: 182-185.

- [7] Wiegand A, Buchalla W, Attin T. Review on fluoridereleasing restorative materials- fluoride release and uptake characteristics, antibacterial activity and influence on caries formation. *Dent Mater* 2007; 23: 343-362.
- [8] Kirsten GA, Rached RN, Mazur RF, Vieira S, Souza EM. Effect of open-sandwich vs. adhesive restorative techniques on enamel and dentine demineralization: an *in situ* study. *J Dent* 2013; 41: 872-880.
- [9] Zhou J, Watanabe S, Watanabe K, Wen LY, Xuan K. *In vitro* study of the effects of fluoride-releasing dental materials on remineralization in an enamel erosion model. *J Dent* 2012; 40: 255-263
- [10] Mickenautsch S, Mount G, Yengopal V. Therapeutic effect of glass-ionomers: an overview of evidence. *Aust Dent J* 2011; 56: 10-15.
- [11] Ten Cate JM. *In vitro* studies on the effects of fluoride on demand remineralization. *J Dent Res* 1990; 69: 614-619.
- [12] Nakajo K, Imazato S, Takahashi Y, Kiba W, Ebisu S, Takahashi N. Fluoride released from glass-ionomer cement is responsible to inhibit the acid production of caries-related oral streptococci. *Dent Mater* 2009; 25: 703-708.

- [13] Prati C, Fava F, Di Gioia D, Selighini M, Pashley DH. Antibacterial effectiveness of dentin bonding systems. *Dent Mater* 1993; 9: 338-343.
- [14] Hallgren A, Oliveby A, Twetman S. Fluoride concentration in plaque adjacent to orthodontic appliances retained with glass ionomer cement. *Caries Res* 1993; 27: 51-54.
- [15] Loyola-Rodriguez JP, Garcia-Godoy F, Lindquist R. Growth inhibition of glass ionomer cements on mutans streptococci. *Pediatr Dent* 1994; 16: 346-349.
- [16] Meiers JC, Miller GA. Antibacterial activity of dentin bonding systems, resin-modified glass ionomers, and polyacid-modified composite resins. *Oper Dent* 1996; 21: 257-264.
- [17] Takahashi Y, Imazato S, Kaneshiro AV, Ebisu S, Frencken JE, Tay FR. Antibacterial effects and physical properties of glass-ionomer cements containing chlorhexidine for the ART approach. *Dent Mater* 2006; 22: 647-652.
- [18] Frencken JE, Imazato S, Toi C, Mulder J, Mickenautsch S, Takahashi Y, Ebisu S. Antibacterial effect of chlorhexidine containing glass ionomer cement *in vivo*: a pilot study. *Caries Res* 2007; 41: 102-107.

- [19] Hoszek A, Ericson D. *In vitro* fluoride release and the antibacterial effect of glass ionomers containing chlorhexidine gluconate. *Oper Dent* 2008; 33: 696-701.
- [20] Türkün LS, Türkün M, Ertuğrul F, Ateş M, Brugger S. Long-term antibacterial effects and physical properties of a chlorhexidine-containing glass ionomer cement. *J Esthet Restor Dent* 2008; 20: 29-45.
- [21] Ersin NK, Uzel A, Aykut A, Candan U, Eronat C. Inhibition of cultivable bacteria by chlorhexidine treatment of dentin lesions treated with the ART technique. *Caries Res* 2006; 40: 172-177.
- [22] Xie D, Weng Y, Guo X, Zhao J, Gregory RL, Zheng C. Preparation and evaluation of a novel glass-ionomer cement with antibacterial functions. *Dent Mater* 2011; 27: 487-496.
- [23] Paiva L, Fidalgo TKS, da Costa LP, Maia LC, Balan L, Anselme K, Ploux L, Thiré RMSM. Antibacterial properties and compressive strength of new one-step preparation silver nanoparticles in glass ionomer cements (NanoAg-GIC). *J Dent* 2018; 69: 102-109.
- [24] Hu J, Du X, Huang C, Fu D, Ouyang X, Wang Y. Antibacterial and physical properties of EGCG-containing glass ionomer cements. *J Dent* 2013; 41: 927-934.

- [25] Elgamily H, Ghallab O, El-Sayed H, Nasr M. Antibacterial potency and fluoride release of a glass ionomer restorative material containing different concentrations of natural and chemical products: an *in vitro* comparative study. *J Clin Exp Dent* 2018; 10: e312-320.
- [26] Lamont RJ, Koo H, Hajishengallis G. The oral microbiota: dynamic communities and host interactions. *Nat Rev Microbiol* 2018, 16: 745-759.
- [27] Radaic A, Kapila Y L. The oralome and its dysbiosis: New insights into oral microbiome-host interactions. *Comput Struct Biotechnol J* 2021; 19: 1335-1360
- [28] Imazato S, Kohno T, Tsuboi R, Thongthai P, Xu HH, Kitagawa H. Cutting-edge filler technologies to release bio-active components for restorative and preventive dentistry. *Dent Mater J* 2020; 39: 69-79.
- [29] Boyd D, Li H, Tanner DA, Towler MR, Wall JG. The antibacterial effects of zinc ion migration from zinc-based glass polyalkenoate cements. *J Mater Sci Mater Med* 2006; 17: 489-494.
- [30] Takatsuka T, Tanaka K, Iijima Y. Inhibition of dentine demineralization by zinc oxide: *in vitro* and *in situ* studies. *Dent Mater* 2005; 21: 1170-1177.

- [31] Abou Neel EA, Aljabo A, Strange A, Ibrahim S, Coathup M, Young AM, Bozec L, Mudera V. Demineralization-remineralization dynamics in teeth and bone. *Int J Nanomed* 2016; 11: 4743-4763.
- [32] He G, Pearce EI, Sissons CH. Inhibitory effect of ZnCl₂ on glycolysis in human oral microbes. *Arch Oral Biol* 2002; 47: 117-129.
- [33] Hasegawa T, Takenaka S, Ohsumi T, Ida T, Ohshima H, Terao Y, Naksagoon T, Maeda T, Noiri Y. Effect of a novel glass ionomer cement containing fluoro-zinc-silicate fillers on biofilm formation and dentin ion incorporation. *Clin Oral Invest* 2020; 24: 963-970.
- [34] Saad A, Nikaido T, Abdou A, Matin K, Burrow MF, Tagami J. Inhibitory effect of zinc containing desensitizer on bacterial biofilm formation and root dentin demineralization. *Dent Mater J* 2019; 38: 940-946.
- [35] Hench LH. The story of bioglass. *J Mater Sci Mater Med* 2006; 17: 967-978.
- [36] Lizzi F, Villat C, Attik N, Jackson P, Grosgeat B, Goutaudier C. Mechanical characteristic and biological behaviour of implanted and restorative bioglasses used in medicine and dentistry: a systematic review. *Dent Mater* 2017; 33: 702-712.

- [37] Tezvergil-Mutluay A, Seseogullari-Dirihan R, Feitosa VP, Cama G, Brauer DS, Sauro S. Effects of composites containing bioactive glasses on demineralized dentin. *J Dent Res* 2017; 96: 999-1005.
- [38] Gubler M, Brunner TJ, Zehnder M, Waltimo T, Sener B, Stark WJ. Do bioactive glasses convey a disinfecting mechanism beyond a mere increase in pH? *Int Endod J* 2008; 41: 670-678.
- [39] Galarraga-Vinueza ME, Passoni B, Benfatti CAM, Mesquita Guimarães J, Henriques B, Magini RS, Fredel MC, Meerbeek BV, Teughels W, Souza JCM. Inhibition of multi-species oral biofilm by bromide doped bioactive glass. *J Biomed Mater Res A* 2017; 105: 1994-2003.
- [40] Moreau JL, Sun L, Chow LC, Xu HH. Mechanical and acid neutralizing properties and bacteria inhibition of amorphous calcium phosphate dental nanocomposite. *J Biomed Mater Res B Appl Biomater* 2011; 98: 80-88.
- [41] Davis HB, Gwinner F, Mitchell JC, Ferracane JL. Ion release from, and fluoride recharge of a composite with a fluoride containing bioactive glass. *Dent Mater* 2014; 30: 1187-1194.

- [42] Tong Z, Tao R, Jiang W, Li J, Zhou L, Tian Y, Ni L. *In vitro* study of the properties of *Streptococcus mutans* in starvation conditions. Arch Oral Biol 2011; 56: 1306-1311.
- [43] Øysæd H, Ruyter IE. Water sorption and filler characteristics of composites for use in posterior teeth. J Dent Res 1986; 65: 1315-1318.
- [44] Gandolfi MG, Chersoni S, Acquaviva GL, Piana G, Prati C, Mongiorgi R. Fluoride release and absorption at different pH from glass-ionomer cements. Dent Mater 2006; 22: 441-449.
- [45] Kavaloglu Cildir S, Sandalli N. Compressive strength, surface roughness, fluoride release and recharge of four new fluoride releasing fissure sealants. Dent Mater J 2007; 26: 335-341.
- [46] Markovic DLj, Petrovic BB, Peric TO. Fluoride content and recharge ability of five glass ionomer dental materials. BMC Oral Health 2008; 8: 21.
- [47] Harrap GJ, Saxton CA, Best JS. Inhibition of plaque growth by zinc salts. J Periodont Res 1983; 18: 634-642.

- [48] Eisenberg AD, Young DA, Fan-Hsu J, Spitz LM. Interactions of sanguinarine and zinc on oral streptococci and *Actinomyces* species. *Caries Res* 1991; 25: 185-190.
- [49] Hernández-Sierra JF, Ruiz F, Pena DCC, Martínez-Gutiérrez F, Martínez AE, Guillén ADJP, Tapia-Pérez H, Castañón GM. The antimicrobial sensitivity of *Streptococcus mutans* to nanoparticles of silver, zinc oxide, and gold. *Nanomedicine* 2008; 4: 237-240.
- [50] Pizzey RL, Marquis RE, Bradshaw DJ. Antimicrobial effects of o-cymen-5-ol and zinc, alone & in combination in simple solutions and toothpaste formulations. *Int Dent J* 2011; 61: 33-40.
- [51] Siqueira Jr JF, Lopes HP. Mechanisms of antimicrobial activity of calcium hydroxide: a critical review. *Int End J* 1999; 32: 361-369.
- [52] Haenni S, Schmidlin PR, Mueller B, Sener B, Zehnder M. Chemical and antimicrobial properties of calcium hydroxide mixed with irrigating solutions. *Int End J* 2003; 36: 100-105.
- [53] Wong L, Sissons CH, Pearce EIF, Cutress TW. Calcium phosphate deposition in human dental plaque microcosm biofilms induced by a ureolytic pH-rise procedure. *Arch Oral Biol* 2002; 47: 779-790.

- [54] Kanapka JA, Hamilton IR. Fluoride inhibition of enolase activity *in vivo* and its relationship to the inhibition of glucose-6-P formation in *Streptococcus salivarius*. Arch Biochem Biophys 1971; 146: 167-174.
- [55] Kitagawa H, Miki-Oka S, Mayanagi G, Abiko Y, Takahashi N, Imazato S. Inhibitory effect of resin composite containing S-PRG filler on *Streptococcus mutans* glucose metabolism. J Dent 2018; 70: 92-96.
- [56] Ishiguro T, Mayanagi G, Azumi M, Otani H, Fukushima A, Sasaki K, Takahashi N. Sodium fluoride and silver diamine fluoride-coated tooth surfaces inhibit bacterial acid production at the bacteria/tooth interface. J Dent 2019; 84: 30-35.
- [57] Takahashi N, Washio J. Metabolomic effects of xylitol and fluoride on plaque biofilm *in vivo*. J Dent Res 2011; 90: 1463-1468.
- [58] Azam A, Ahmed AS, Oves M, Khan MS, Habib SS, Memic A. Antimicrobial activity of metal oxide nanoparticles against Gram-positive and Gram-negative bacteria: a comparative study. Int J Nanomed 2012; 7: 6003-6009.
- [59] Joo JH, Hassan SHA, Oh SE. Comparative study of biosorption of Zn²⁺ by *Pseudomonas aeruginosa* and *Bacillus cereus*. Int Biodeterior & Biodegradation 2010; 64: 734-741.

- [60] Naskar A, Lee S, Kim K. Antibacterial potential of Ni-doped zinc oxide nanostructure: Comparatively more effective against Gram-negative bacteria including multi-drug resistant strains. *RSC Adv* 2020; 10: 1232-1242.
- [61] Mehmood S, Rehman MA, Ismail H, Mirza B, Bhatti AS. Significance of postgrowth processing of ZnO nanostructures on antibacterial activity against gram-positive and gram-negative bacteria. *Int J Nanomed* 2015; 10: 4521.
- [62] Rutherford D, Jíra J, Kolářová K , Matolínová I, Mičová J, Remeš Z, Rezek B. Growth inhibition of gram-positive and gram-negative bacteria by zinc oxide hedgehog particles. *Int J Nanomed* 2021; 16: 3541.
- [63] Ishida ST. Bacteriolyses of bacterial cell walls by Cu (II) and Zn (II) ions based on antibacterial results of dilution medium method and halo antibacterial test. *J Adv Res Biotech* 2017; 2: 1-12.
- [64] Vinopal S, Ruml T, Kotrba P. Biosorption of Cd²⁺ and Zn²⁺ by cell surface-engineered *Saccharomyces cerevisiae*. *Int Biodeterior Biodegradation* 2007; 60: 96-102.

- [65] Lee SF. Identification and characterization of a surface protein-releasing activity in *Streptococcus mutans* and other pathogenic streptococci. *Infect and Immun* 1992; 60: 4032-4039.
- [66] Cummins D. Zinc citrate/Triclosan: a new anti-plaque system for the control of plaque and the prevention of gingivitis: short-term clinical and mode of action studies. *J Clin Periodontol* 1991; 18: 455-461.
- [67] Jin G, Cao H, Qiao Y, Meng F, Zhu H, Liu X. Osteogenic activity and antibacterial effect of zinc ion implanted titanium. *Colloids Surf B Biointerfaces* 2014; 117: 158-165.
- [68] Cagetti MG, Campus G, Sale S, Cocco F, Strohmer L, Lingström P. Association between interdental plaque acidogenicity and caries risk at surface level: a cross sectional study in primary dentition. *Int J Paediatr Dent* 2011; 21: 119-125.
- [69] Geddes DAM. Acids produced by human dental plaque metabolism *in situ*. *Caries Res* 1975; 9: 98-109.
- [70] De Soet JJ, Nyvad B, Kilian M. Strain-related acid production by oral streptococci. *Caries Res* 2000; 34: 486-490.

- [71] Bingel L, Groh D, Karpukhina N, Brauer DS. Influence of dissolution medium pH on ion release and apatite formation of Bioglass[®] 45S5. *Mater Lett* 2015; 143: 279-282.
- [72] Sepulveda P, Jones JR, Hench LL. *In vitro* dissolution of melt-derived 45S5 and sol-gel-derived 58S bioactive glasses. *J Biomed Mater Res A* 2002; 61: 301-311.
- [73] Wasson EA, Nicholson JW. Studies on the setting chemistry of glass-ionomer cements. *Clin Mater* 1991; 7: 289-293.
- [74] Griffin SG, Hill RG. Influence of glass composition on the properties of glass polyalkenoate cements. Part I: influence of aluminium to silicon ratio. *Biomaterials* 1999; 20: 1579-1586.
- [75] Schepers EJG, Ducheyne P. Bioactive glass particles of narrow size range for the treatment of oral bone defects: a 1–24 month experiment with several materials and particle sizes and size ranges. *J Oral Rehabil* 1997; 24: 171-181.
- [76] Zhong J, Greenspan DC. Processing and properties of sol–gel bioactive glasses. *J Biomed Mater Res A* 2000; 53: 694-701.

- [77] Nicholson JW. Chemistry of glass-ionomer cements: a review. *Biomaterials* 1998; 19: 485-494.
- [78] Wilson AD, Crisp S, Ferner AJ. Reactions in glass-ionomer cements: IV. Effect of chelating comonomers on setting behavior. *J Dent Res* 1976; 55: 489-495.
- [79] Sidhu SK, Nicholson JW. A review of glass-ionomer cements for clinical dentistry. *J Funct Biomater* 2016; 7: 16.
- [80] Stephan RM. Intra-oral hydrogen-ion concentrations associated with dental caries activity. *J Dent Res* 1944; 23: 257-266.
- [81] Sönmez IŞ, Aras Ş. Effect of white cheese and sugarless yoghurt on dental plaque acidogenicity. *Caries Res* 2007; 41: 208-211.
- [82] Igarashi K, Lee IK, Schachtele CF. Effect of dental plaque age and bacterial composition on the pH of artificial fissures in human volunteers. *Caries Res* 1990; 24: 52-58.
- [83] Kolenbrander PE, Palmer RJ Jr, Rickard AH, Jakubovics NS, Chalmers NI, Diaz PI. Bacterial interactions and successions during plaque development. *Periodontol* 2000 2006; 42: 47-79.

- [84] He Z, Huang Z, Zhou W, Tang Z, Ma R, Liang J. Anti-biofilm activities from resveratrol against *Fusobacterium nucleatum*. *Front Microbiol* 2016; 7: 1065.
- [85] Ghasempour M, Rajabnia R, Irannejad A, Hamzeh M, Ferdosi E, Bagheri M. Frequency, biofilm formation and acid susceptibility of *Streptococcus mutans* and *Streptococcus sobrinus* in saliva of preschool children with different levels of caries activity. *J Dent Res* 2013; 10: 440-445.
- [86] Jordan HV, Hammond BF. Filamentous bacteria isolated from human root surface caries. *Arch Oral Biol* 1972; 17: 1333-1342.
- [87] Bowden GHW. Microbiology of root surface caries in humans. *J Dent Res* 1990; 69: 1205-1210.
- [88] Kolenbrander PE, Andersen RN, Blehert DS, Egland PG, Foster JS, Palmer RJ Jr. Communication among oral bacteria. *Microbiol Mol Biol Rev* 2002; 66: 486-505.
- [89] Wake N, Asahi Y, Noiri Y, Hayashi M, Motooka D, Nakamura S, Gotoh K, Miura J, Machi H, Iida T, Ebisu S. Temporal dynamics of bacterial microbiota in the human oral cavity determined using an *in situ* model of dental biofilms. *NPJ Biofilms Microbiomes* 2016; 2: 1-9.

- [90] Sotozono M, Kuriki N, Asahi Y, Noiri Y, Hayashi M, Motooka D, Nakamura S, Machi H, Iida T, Ebisu S. Impacts of sleep on the characteristics of dental biofilm. *Sci Rep* 2021; 11: 1-12.
- [91] Ccahuana-Vásquez RA, Cury JA. *S. mutans* biofilm model to evaluate antimicrobial substances and enamel demineralization. *Braz Oral Res* 2010; 24: 135-141.
- [92] Banas JA. Virulence properties of *Streptococcus mutans*. *Front Biosci* 2004; 9: 1267-1277.
- [93] Dang MH, Jung JE, Choi HM, Jeon JG. Difference in virulence and composition of a cariogenic biofilm according to substratum direction. *Sci Rep* 2018; 8: 6244.
- [94] Surmount PA, Martens LC. Root surface caries: an update. *Clin Prev Dent* 1989; 11: 14-20.
- [95] Heijnsbroek M, Paraskevas S, Van der Weijden GA. Fluoride interventions for root caries: a review. *Oral Health Prev Dent* 2007; 5: 145-152.
- [96] Kaneshiro AV, Imazato S, Ebisu S, Tanaka S, Tanaka Y, Sano H. Effects of a self-etching resin coating system to prevent demineralization of root surfaces. *Dent Mater* 2008; 24: 1420-1427.

- [97] Takahashi K, Shimada Y, Tagami J, Yoshiyama M. The effects of root demineralization inhibition by a glass ionomer cement containing zinc glass. *Jpn J Conserv Dent* 2019; 62: 190-198.
- [98] Mohammed NR, Mneimne M, Hill RG, Al-Jawad M, Lynch RJM, Anderson P. Physical chemical effects of zinc on *in vitro* enamel demineralization. *J Dent* 2014; 42: 1096-1104.
- [99] Takatsuka T, Tanaka K, Iijima Y. Inhibition of dentine demineralization by zinc oxide: *in vitro* and *in situ* studies. *Dent Mater* 2005; 21: 1170-1177.
- [100] Bowen WH. The Stephan Curve revisited. *Odontology*. 2013; 101: 2-8.
- [101] Golub LM, Borden SM, Kleinberg I. Urea content of gingival crevicular fluid and its relation to periodontal diseases in humans. *J Periodontal Res* 1971; 6: 243-251.
- [102] Burne RA, Marquis RE. Alkali production by oral bacteria and protection against dental caries. *FEMS Microbiol Lett* 2000; 193: 1-6.
- [103] ISO 9917-1; 2007 Dentistry–Water-based cements–Part 1: Powder/liquid acid-base cements.

- [104] Sawa N. The effect of filler shape and size of resin composite on fracture toughness. *J Jpn Conser Dent* 1993; 36: 507-518.
- [105] Moheet IA, Luddin N, Rahman IA, Kannan TP, Nik Abd Ghani NR, Masudi SM. Modifications of glass ionomer cement powder by addition of recently fabricated nano- fillers and their effect on the properties: a review. *Eur J Dent* 2019; 13: 470-477.
- [106] Crisp S, Lewis BG, Wilson AD. Characterization of glass-ionomer cements. I. Long-term hardness and compressive strength. *J Dent* 1976; 4: 162-166.
- [107] Moshaverinia A, Ansari S, Moshaverinia M, Roohpour N, Darr JA, Rehman I. Effects of incorporation of hydroxyapatite and fluoroapatite nanobioceramics into conventional glass ionomer cements (GIC). *Acta Biomater* 2008; 4: 432-440.

TABLE LEGENDS

Table 1. Compositions of glass powder tested.

Table 2. Bacteria and culture conditions.

Table 3. Elemental composition of BU.

Table 4. Concentrations of Zn^{2+} , Ca^{2+} , and F^{-} released from BU and F7 powder into distilled water and acetic acid.

Table 5. Minimum inhibitory concentrations (MICs) and minimum bactericidal concentrations (MBCs) of Zn^{2+} , Ca^{2+} , and F^{-} .

Table 6. GIC and resin composites used.

Table 7. Release of Zn^{2+} , Ca^{2+} , and F^{-} from CA and F7 into water and acetic acid within 24 h.

Table 8. Elemental composition of CA.

Table 9. Physical properties and their bond strength to enamel and dentin of CA and F7.

FIGURE LEGENDS

Figure 1. Schematic diagram of acidity-induced release of zinc ion from the restorative material containing BioUnion filler and exhibition of antibacterial effect.

Figure 2. BioUnion filler (BU).

A: Appearance

B: : Field-emission scanning electron microscope image of BU

Figure 3. The protocol for the evaluation of ion release from BU.

Figure 4. The protocol for the evaluation of Zn²⁺-release from BU with repeated exposure to acid.

Figure 5. The protocol to assess the inhibition of *S. mutans* by BU with repeated exposure to acid.

Figure 6. Elemental mapping images of BU.

Figure 7. Solubilities of BU and F7 powder into acetic acid and distilled water.

Bars represent the standard deviation of three replicates. a-c; Different letters indicate significant differences ($p < 0.05$, ANOVA, Tukey's HSD test).

Figure 8. XRD patterns of BU after immersion in distilled water (A), acetic acid (B), and hydrochloric acid (C).

▼; Peak positions were matched with LaF_3 of the standard material in the powder diffraction file of the International Center for Diffraction Data 2013.

Figure 9. Number of viable *S. mutans* after incubation in the presence of BU and F7 powder.

Sc (-): bacterial suspension without sucrose. Sc (+): bacterial suspension with 1% sucrose. Control: bacterial suspension without any particles.

Bars represent the standard deviation of three replicates. Different letters (a–f) indicate significant differences ($p < 0.05$, ANOVA, Tukey's HSD test).

Figure 10. Release profile of Zn²⁺ from BU subjected to repeated exposure to acid (A) and inhibition of *S. mutans* (B).

A: Release profiles of Zn²⁺ from BU into acetic acids (pH 4.5/5.5) on Days 0–1, Days 4–5, and Days 8–9 and into distilled water (pH7.0) on Days 1–4, Days 5–8, and Days 9–10. Bars represent the standard deviation of five replicates.

B: Number of viable bacteria in the presence of BU on Day 8 (after two exposure to acetic acid at pH 4.5) using the same method as (A). Control: bacterial suspension without any particles. Bars represent the standard deviation of three replicates. ** indicate significant differences ($p < 0.001$, ANOVA, Tukey's HSD test).

Figure 11. pH change of *S. mutans* suspension after incubation with or without sucrose.

Sc (-): bacterial suspension without sucrose. Sc (+): bacterial suspension with 1% sucrose.

Figure 12. Possible mechanism of the antibacterial action of Zn²⁺.

Zn²⁺ penetrate and disturb the membranes of gram-positive and gram-negative bacteria, or directly alter the proteins via processes such as transmembrane proton translocation.

Figure 13. The protocol for measurement of Zn²⁺ release from CA with repeated expose to acid.

Figure 14. The protocol for antibacterial activity test of CA with repeated exposure to acid.

Figure 15. Custom-made splint and disc-shaped specimens for *in situ* assessments.

Figure 16. Release profile of Zn^{2+} from CA after repeated exposure to acetic acid.

The bars represent the standard deviations of five replicates.

Figure 17. FE-SEM images and elemental mapping images of CA before and after repeated exposure to acetic acid.

Figure 18. Inhibitory effects of CA before and after repeated exposure to acid against the growth of (A) *S. mutans*, (B) *S. sobrinus*, (C) *S. oralis*, (D) *S. mitis*, (E) *A. naeslundii*, and (F) *F. nucleatum*.

The bars represent the standard deviations of five replicates. * indicates significant differences ($p < 0.05$, ANOVA, Tukey's HSD test).

Figure 19. Number of bacteria adhered on CA after incubation for the six bacterial species.

The bars represent the standard deviations of five replicates. * indicates significant differences ($p < 0.05$, ANOVA, Tukey's HSD test)

Figure 20. *In situ* biofilm formation on the surface of each specimen.

(A) CLSM images. (B) Thickness of biofilm analyzed from CLSM images. (C) The number of surviving cells in the biofilm. The bars represent the standard deviations of four replicates. ** indicates significant differences ($p < 0.001$, ANOVA, Tukey's HSD test).

Figure 21. Schematic diagram of reaction of BU in the powder of CA with polyacrylic acid.

Table 1. Compositions of glass powder tested.

Particle	Code	Composition	Median diameter
BioUnion filler	BU	SiO ₂ F CaO ZnO	4.5-5.5 μm
Fuji VII powder	F7 powder	SiO ₂ Al ₂ O ₃ F	1.6-2.6 μm

Table 2. Bacteria and culture conditions.

Species	Broth	Agar	Incubation time	pH after incubation with sucrose
<i>Streptococcus mutnas</i> NCTC10449	BHI*	BHI agar	24 h	4.3
<i>Streptococcus sobrinus</i> NCTC12279				4.2
<i>Streptococcus oralis</i> NCTC11427				4.5
<i>Streptococcus mitis</i> NCTC12261				4.4
<i>Actinomyces naeslundii</i> ATCC19246	BHI	BHI agar	48 h	4.6
<i>Fusobacterium nucleatum</i> 1436	THB** containing 0.1% L-cystein	THB agar containing 0.1% L-cysteine	48 h	4.7

*BHI: brain-heart infusion

**THB: Todd Hewitt broth.

Table 3. Elemental composition of BU.

Element	Mass%	Atom%
Si	9.00±0.04	6.76±0.03
F	5.21±0.04	5.78±0.05
Ca	2.95±0.03	1.55±0.01
Zn	12.69±0.16	4.09±0.05

Table 4. Concentrations of Zn²⁺, Ca²⁺, and F⁻ released from BU and F7 powder into distilled water and acetic acid.

	Distilled water (pH7.0)	Acetic acid (pH5.5)	Acetic acid (pH4.5)
BU			
Zn²⁺	5.9±1.9 ^a	166.9±11.2 ^b	502.8±8.5 ^c
Ca²⁺	1.4±0.4 ^d	24.1±4.7 ^e	102.8±3.5 ^f
F⁻	81.4±2.4 ^g	1.54±0.2 ^h	4.0±0.8 ⁱ
F7 powder			
Zn²⁺	n.d.	n.d.	n.d.
Ca²⁺	n.d.	n.d.	n.d.
F⁻	9.9±0.7 ^j	0.71±0.1 ^k	2.6±0.3 ^l

Mean±S.D. (ppm), n.d.; Not detected, a–l: Different lowercase letters within the same row indicate significant differences ($p < 0.05$, ANOVA, Tukey's HSD test, $n = 5$).

Table 5. Minimum inhibitory concentrations (MICs) and minimum bactericidal concentrations (MBCs) of Zn²⁺, Ca²⁺, and F⁻.

	MICs (ppm)			MBCs (ppm)		
	Zn ²⁺	Ca ²⁺	F ⁻	Zn ²⁺	Ca ²⁺	F ⁻
<i>S. mutans</i>	64	512	128	512	4096	2048
<i>S. sobrinus</i>	128	512	256	2048	8192	4096
<i>S. oralis</i>	64	256	256	1024	8192	8192
<i>S. mitis</i>	64	1024	128	512	8192	1024
<i>A. naeslundii</i>	128	512	256	512	4096	4096
<i>F. nucleatum</i>	128	512	256	1024	2048	2048

Table 6. GIC and resin composites used.

Product	Manufacturer	Code	Component
Caredyne Restore	GC Corp.	CA	Powder: Fluorozincsilicate glass (BU; 35-45%) Fluoroaluminosilicate glass (55-65%)
			Liquid: Polyacrylic acid Polybasic carboxylic acid Distilled water
Fuji VII	GC Corp.	F7	Powder: Fluoroaluminosilicate glass
			Liquid: Polyacrylic acid Polybasic carboxylic acid Distilled water
MI Fil	GC Corp.	MI	UDMA* Bis-MEPP TEGDMA** Silicon dioxide Strontium glass

*UDMA: Urethane dimethacrylate

**TEGDMA: Triethyleneglycol dimethacrylate

Table 7. Release of Zn²⁺, Ca²⁺, and F⁻ from CA and F7 into water and acetic acid within 24 h.

	Water (pH7.0)	Acetic acid (pH4.5)
CA		
Zn²⁺	3.6±0.9 ^a	170.4±7.0 ^b
Ca²⁺	2.7±1.4 ^a	26.4±2.6 ^c
F⁻	160±10.7 ^b	110.2±6.0 ^d
F7		
Zn²⁺	n.d.	n.d.
Ca²⁺	n.d.	n.d.
F⁻	89.9±1.4 ^e	50.8±7.0 ^f

Mean±S.D. (ppm), n.d.; Not detected, a–f: Different lowercase letters within the same row indicate significant differences ($p < 0.05$, ANOVA, Tukey's HSD test, $n = 5$).

Table 8. Elemental composition of CA.

Element	Mass%	Atom%
Si	9.65±0.12	6.75±0.09
F	8.85±0.17	9.15±0.18
Ca	1.55±0.06	0.76±0.03
Zn	5.83±0.33	1.75±0.10

Table 9. Physical properties and bond strength to enamel and dentin of CA and F7.

	CA	F7	Requirements by ISO (9917-1)
Setting time (s)	165	150	90-360
Acid erosion (mm)	0.049 ± 0.007	0.053 ± 0.008	<0.17
Compressive strength (Day 0) (MPa)	146.8 ± 5.2	143.9 ± 8.3	>100
Compressive strength after acid exposure (Day 28) (MPa)	140 ± 10.1	135.5 ± 7.4	
Toothbrush wear (μm)	6.4 ± 5.4	5.4 ± 3.3	
Shear bond strength Enamel (MPa)	5.4 ± 0.8	5.3 ± 1.3	
Shear bond strength Dentin (MPa)	4.7 ± 0.7	4.9 ± 0.9	

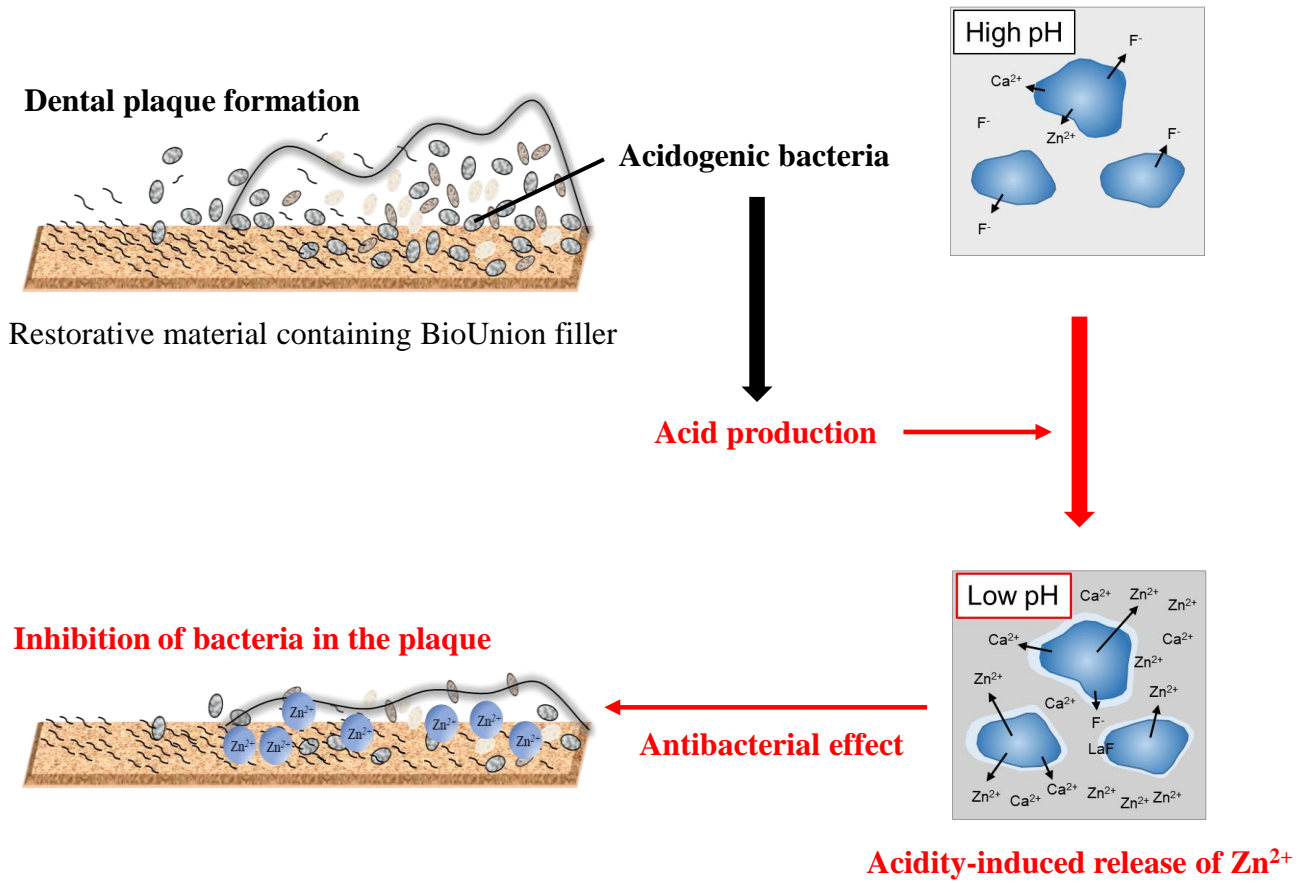
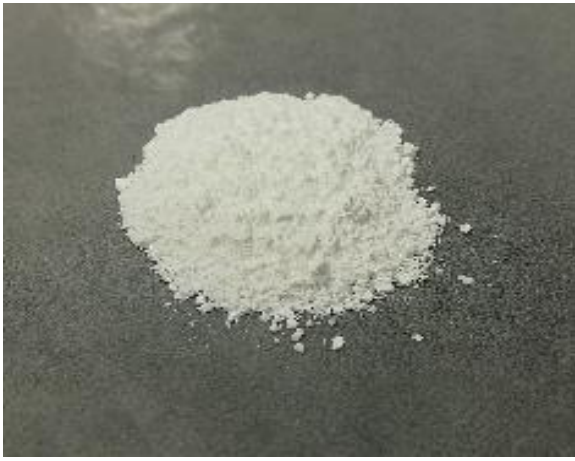


Figure 1. Schematic diagram of acidity-induced release of zinc ion from the restorative material containing BioUnion filler and exhibition of antibacterial effect.

A



B

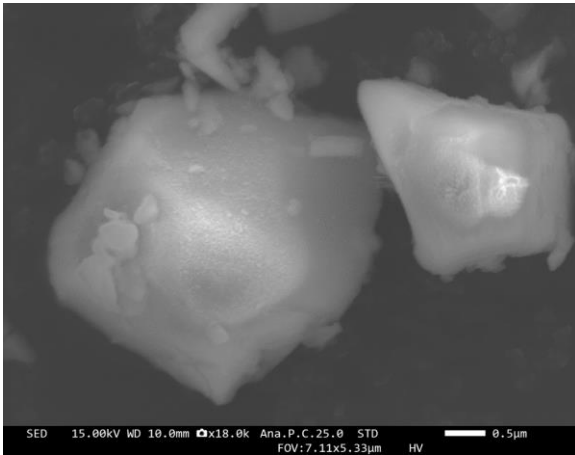


Figure 2. BioUnion filler (BU).

A: Appearance.

B: Field-emission scanning electron microscope image of BU.

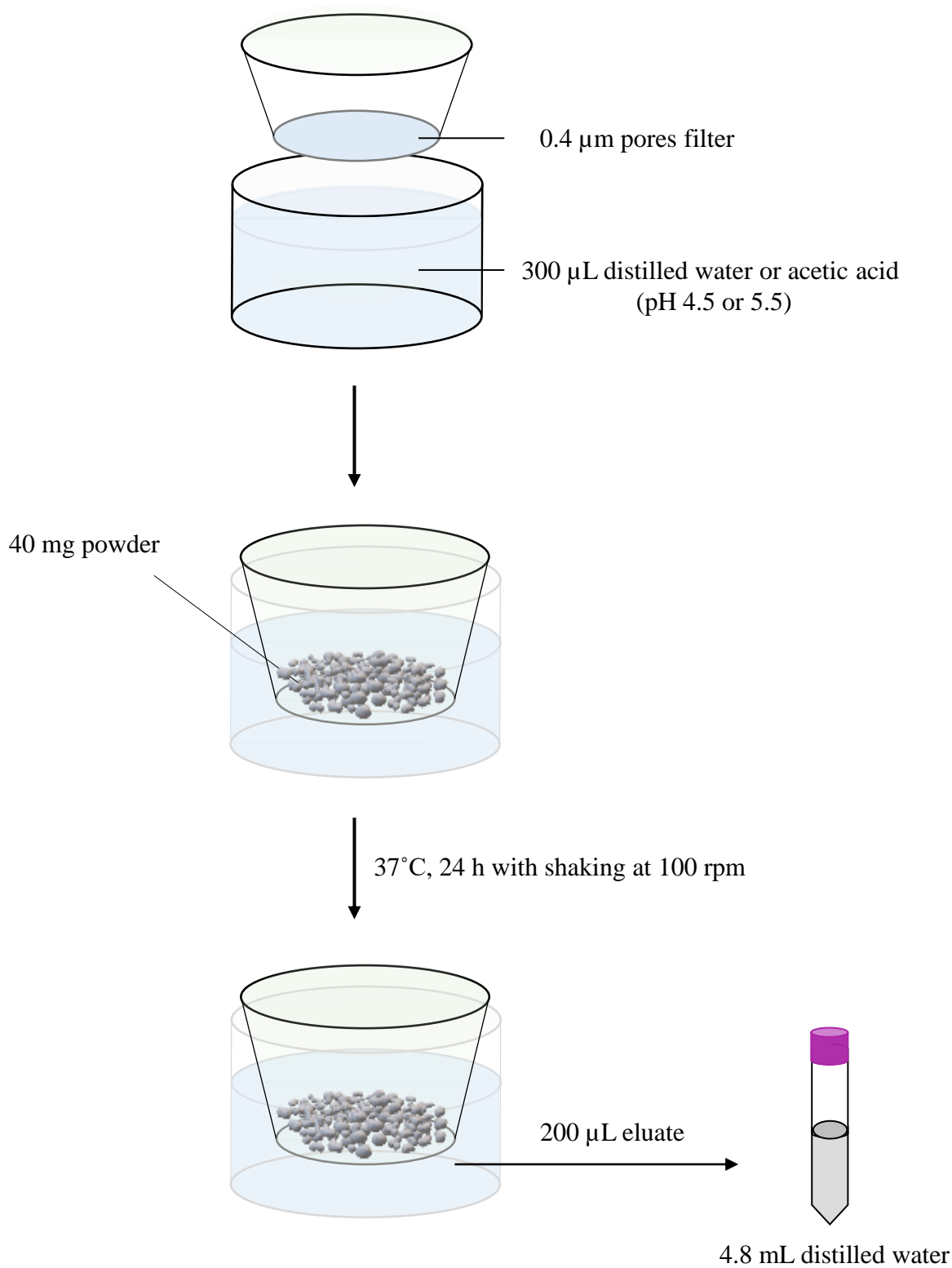


Figure 3. The protocol for the evaluation of ion release from BU.

Day 0-1	Day 1-2	Day 2-3	Day 3-4	Day 4-5	Day 5-6	Day 6-7	Day 7-8	Day 8-9	Day 9-10
Acetic acid (pH 4.5)	Distilled water	Distilled water	Distilled water	Acetic acid (pH 4.5)	Distilled water	Distilled water	Distilled water	Acetic acid (pH 4.5)	Distilled water

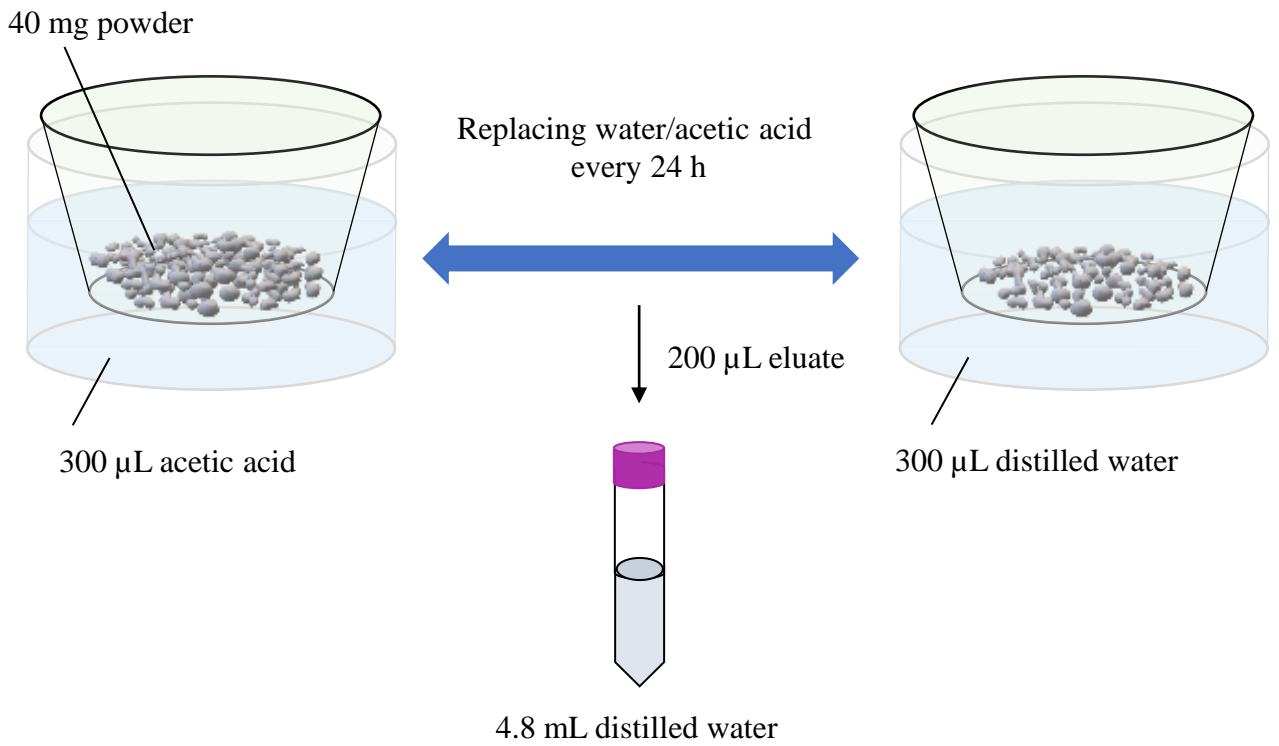


Figure 4. The protocol for the evaluation of Zn²⁺-release from BU with repeated exposure to acid.

Day 0-1	Day 1-2	Day 2-3	Day 3-4	Day 4-5	Day 5-6	Day 6-7	Day 7-8	Day 8-9	Day 9-10
Acetic acid (pH 4.5)	Distilled water	Distilled water	Distilled water	Acetic acid (pH 4.5)	Distilled water	Distilled water	Distilled water	Acetic acid (pH 4.5)	Distilled water


 Day 8

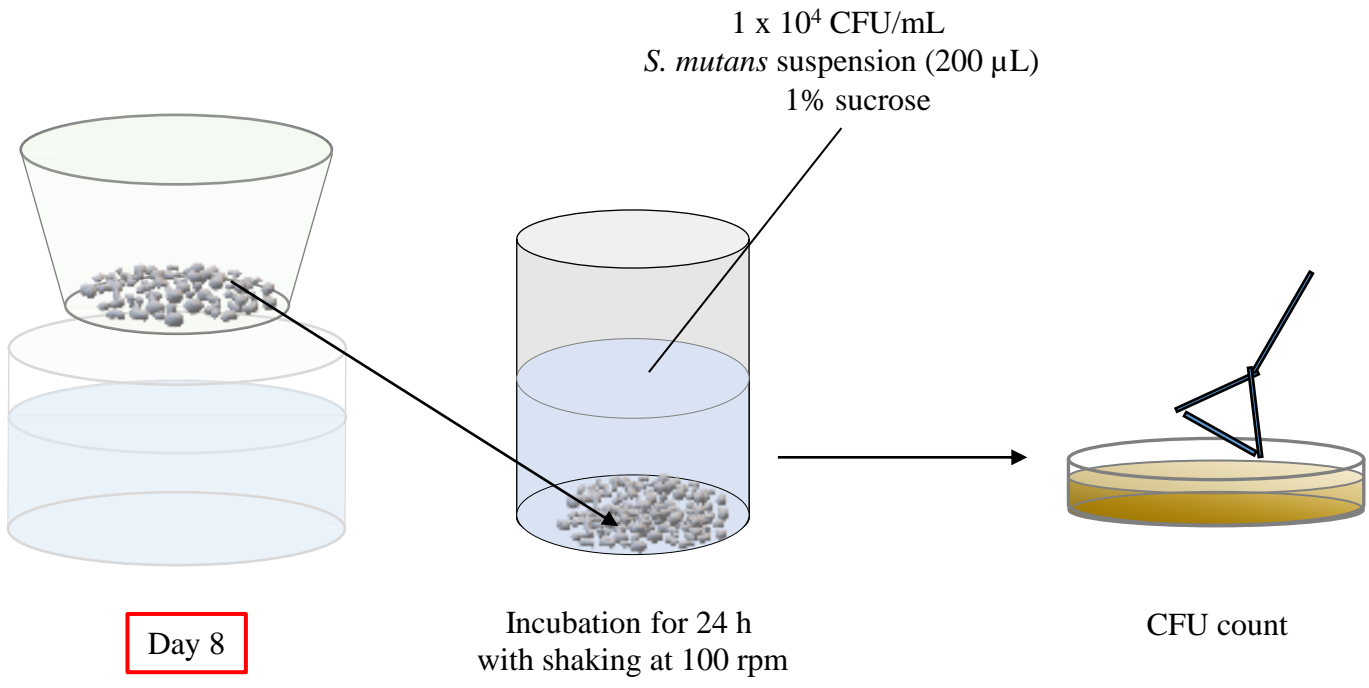


Figure 5. The protocol to assess the inhibition of *S. mutans* by BU with repeated exposure to acid.

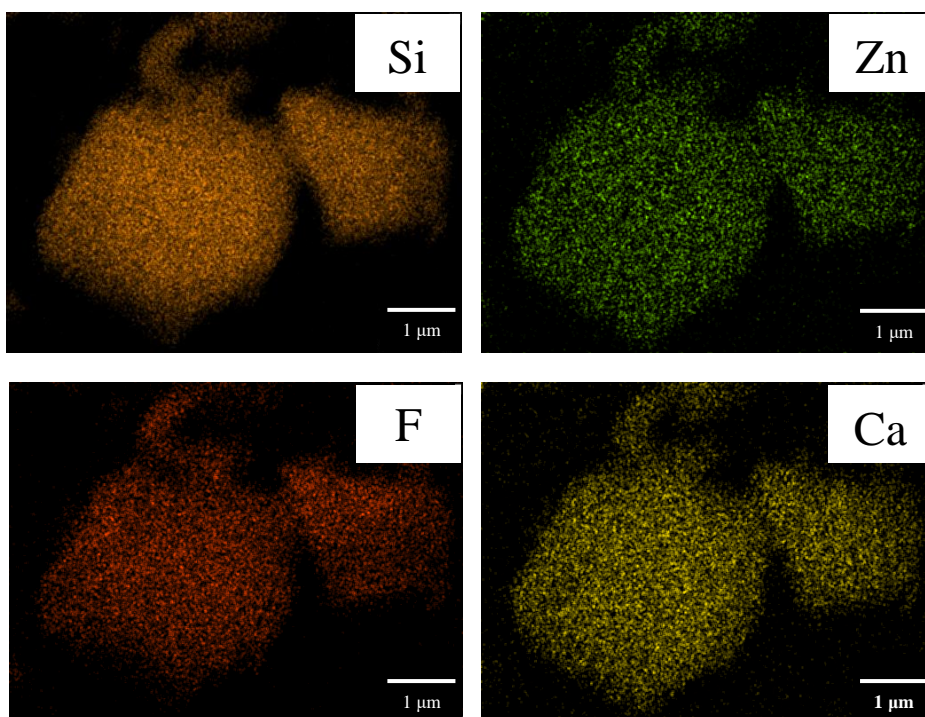


Figure 6. Elemental mapping images of BU.

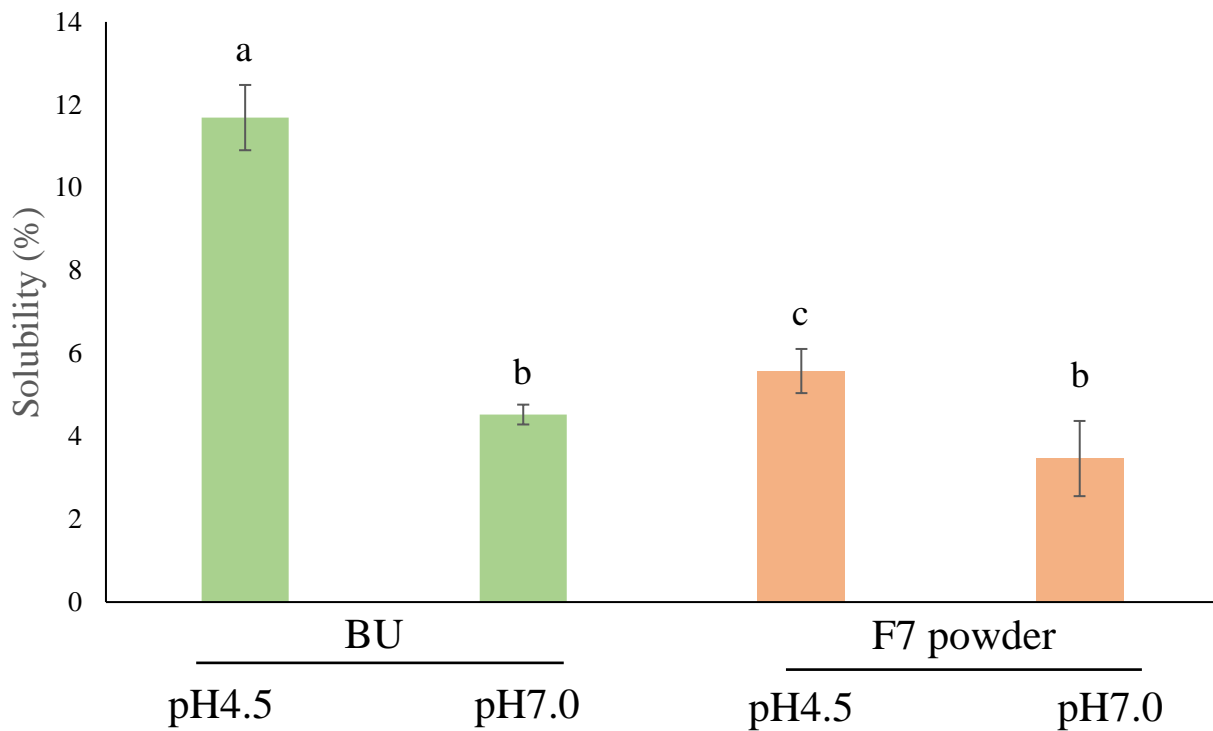


Figure 7. Solubilities of BU and F7 powder into acetic acid and distilled water.

Bars represent the standard deviation of three replicates. a-c; Different letters indicate significant differences ($p < 0.05$, ANOVA, Tukey's HSD test).

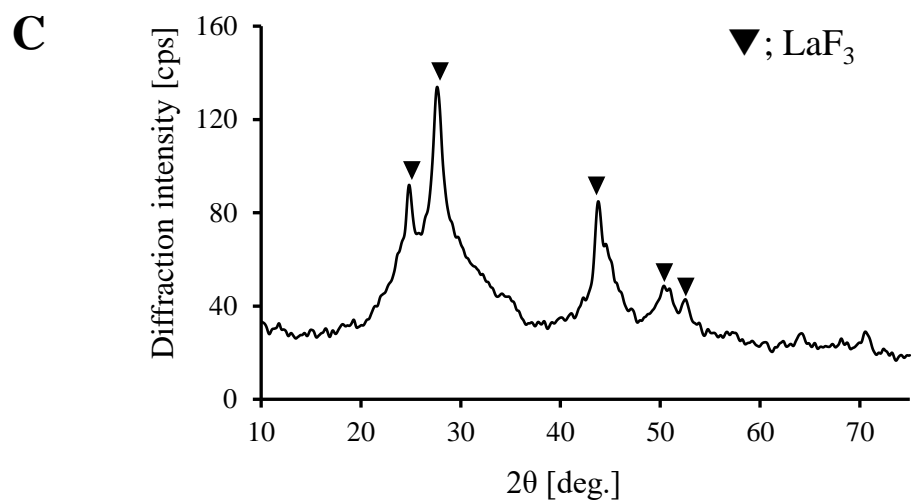
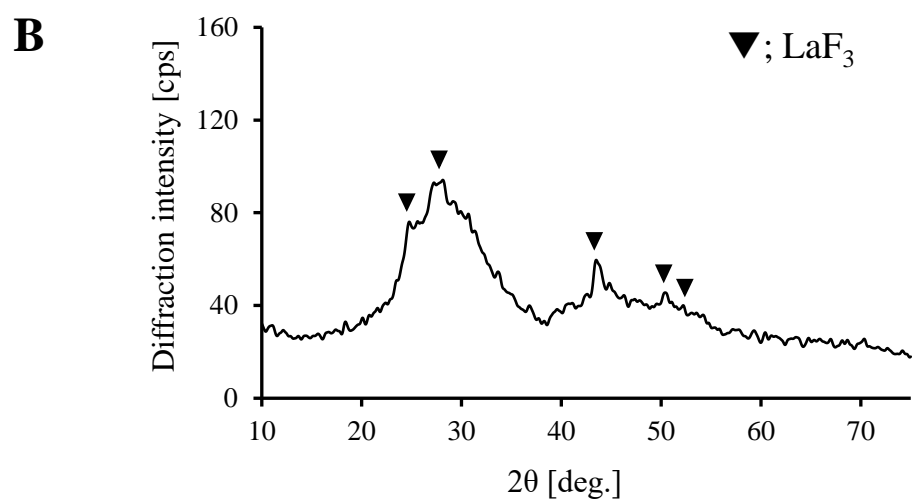
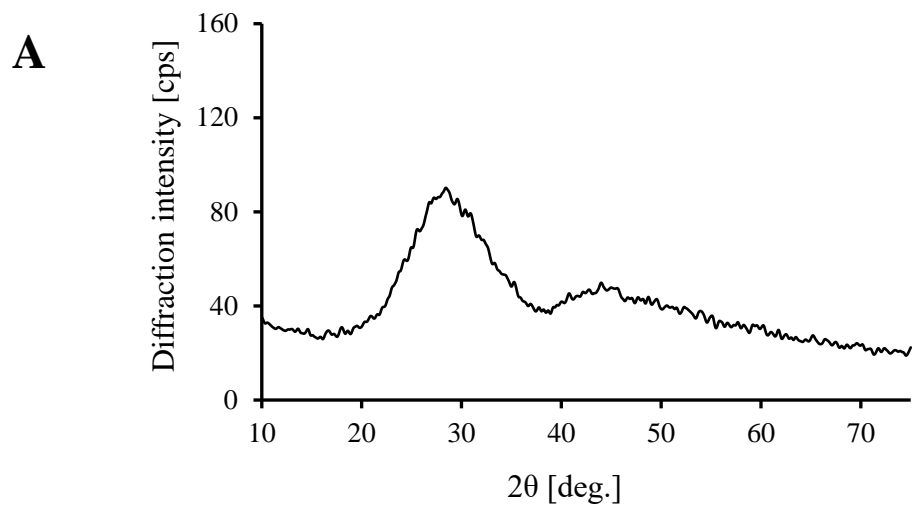


Figure 8. XRD patterns of BU after immersion in distilled water (A), acetic acid (B), and hydrochloric acid (C).

▼; Peak positions were matched with LaF₃ of the standard material in the powder diffraction file of the International Center for Diffraction Data 2013.

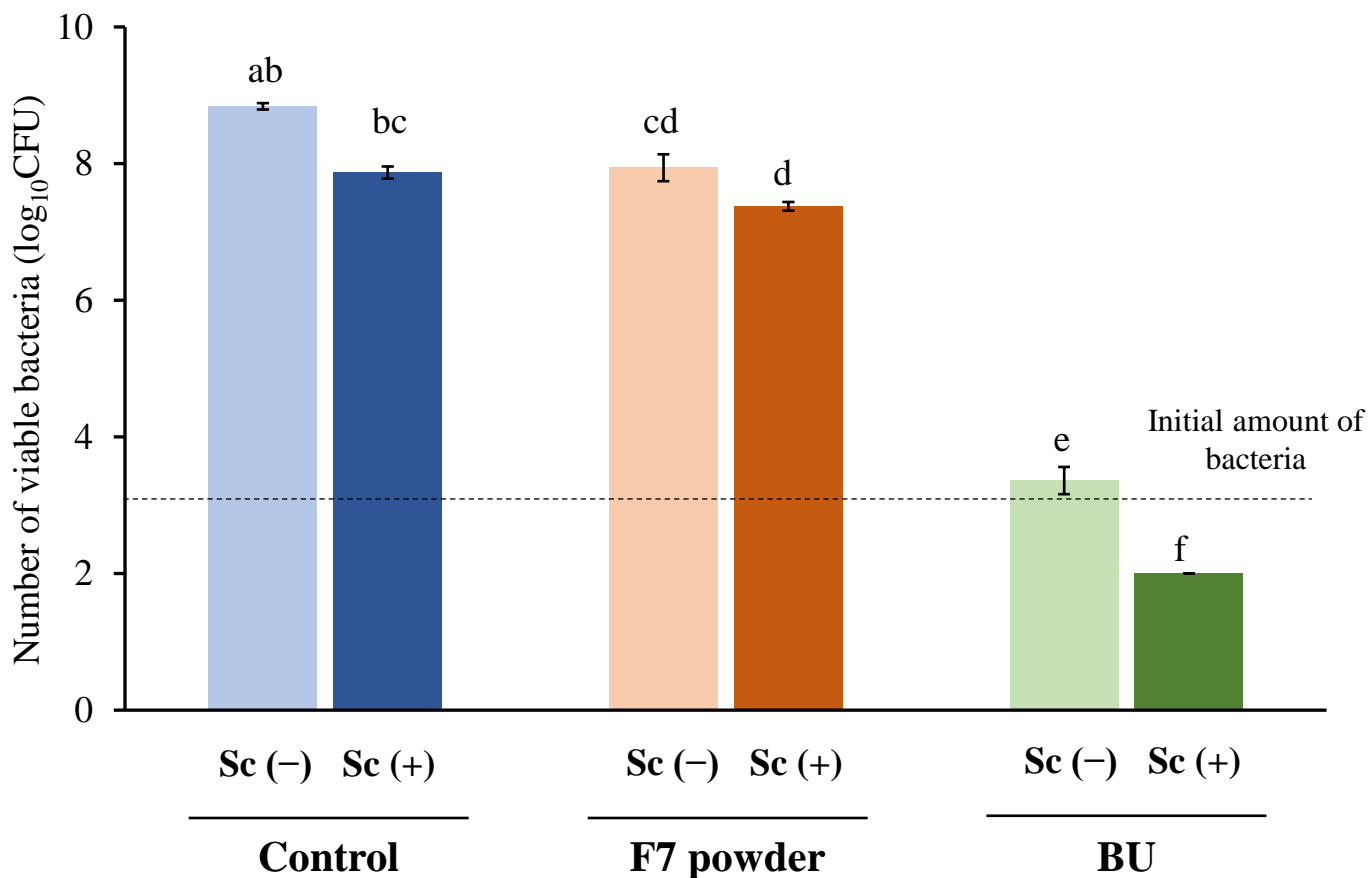


Figure 9. Number of viable *S. mutans* after incubation in the presence of BU and F7 powder.

Sc (-): bacterial suspension without sucrose. Sc (+): bacterial suspension with 1% sucrose.

Control: bacterial suspension without any particles.

Bars represent the standard deviation of three replicates. Different letters (a–f) indicate significant differences ($p < 0.05$, ANOVA, Tukey's HSD test).

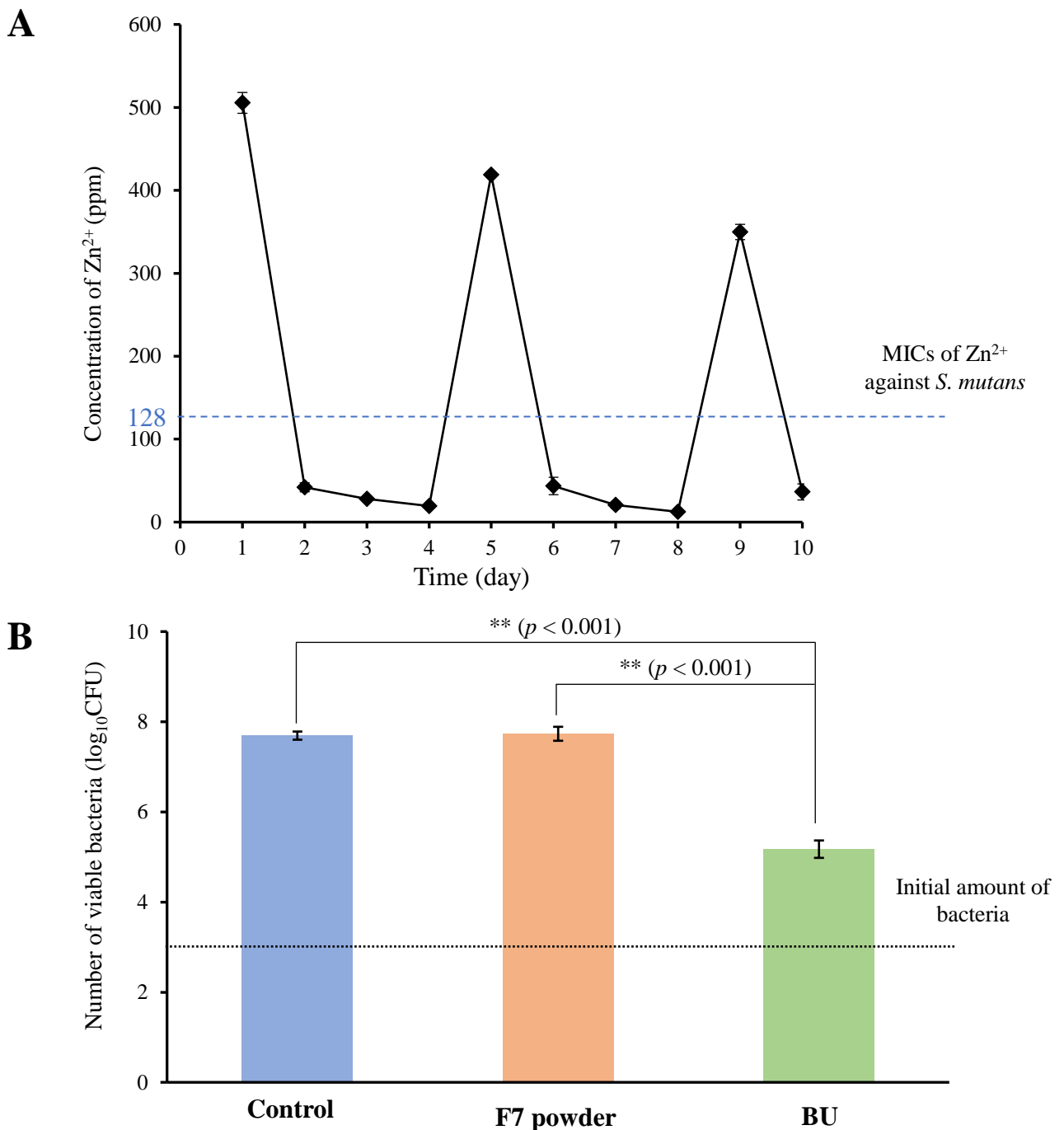


Figure 10. Release profile of Zn²⁺ from BU subjected to repeated exposure to acid (A) and inhibition of *S. mutans* (B).

A: Release profiles of Zn²⁺ from BU into acetic acids (pH 4.5) on Days 0–1, Days 4–5, and Days 8–9 and into distilled water (pH7.0) on Days 1–4, Days 5–8, and Days 9–10.

Bars represent the standard deviation of five replicates.

B: Number of viable bacteria in the presence of BU on Day 8 (after two times exposure to acetic acid at pH 4.5) using the same method as (A). Control: bacterial suspension without any particles.

Bars represent the standard deviation of three replicates. * indicate significant differences ($p < 0.001$, ANOVA, Tukey's HSD test).

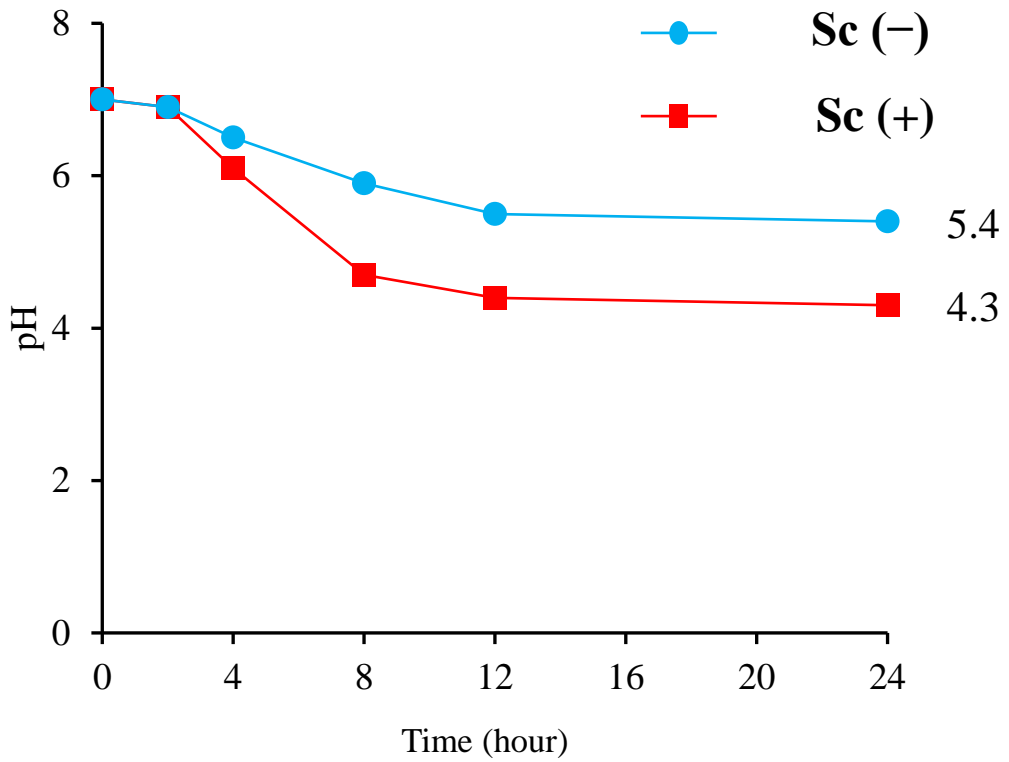


Figure 11. pH change of *S. mutans* suspension after incubation with or without sucrose.

Sc (-): bacterial suspension without sucrose. Sc (+): bacterial suspension with 1% sucrose.

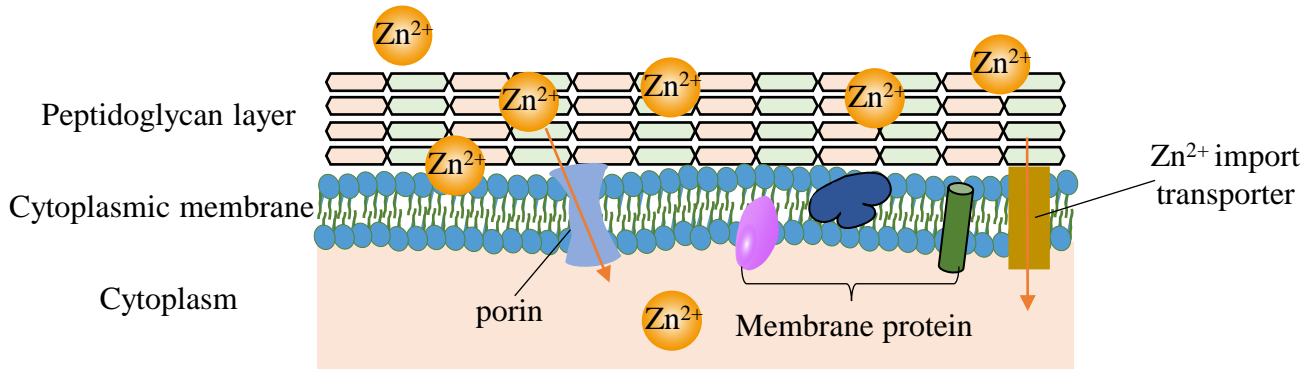
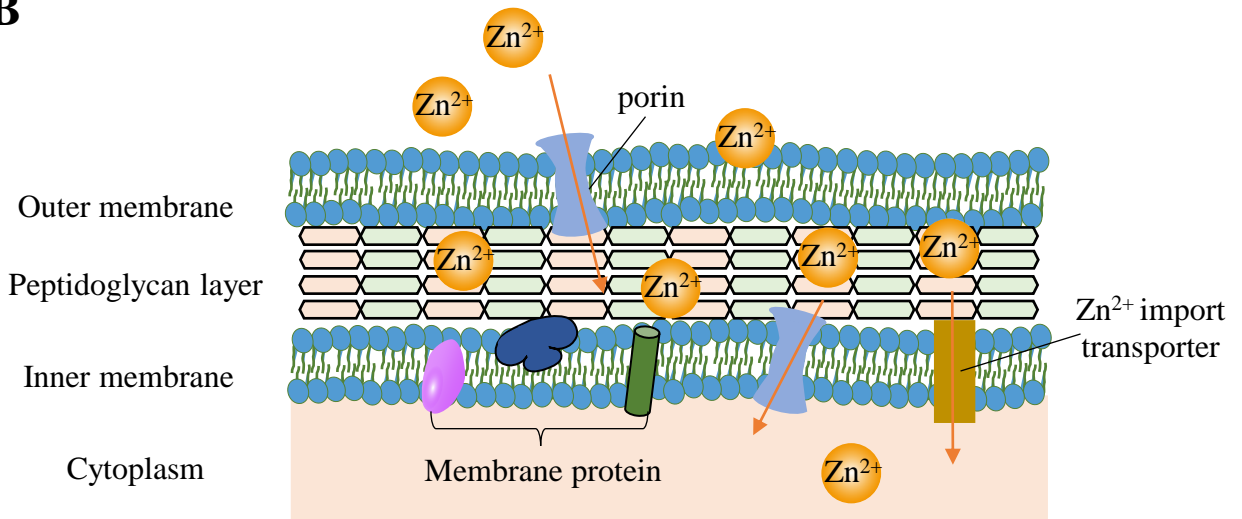
A**gram-positive****B****gram-negative**

Figure 12. Possible mechanism of the antibacterial action of Zn^{2+} .

Zn^{2+} penetrate and disturb the membranes of (A) gram-positive and (B) gram-negative bacteria, or directly alter the proteins via processes such as transmembrane proton translocation.

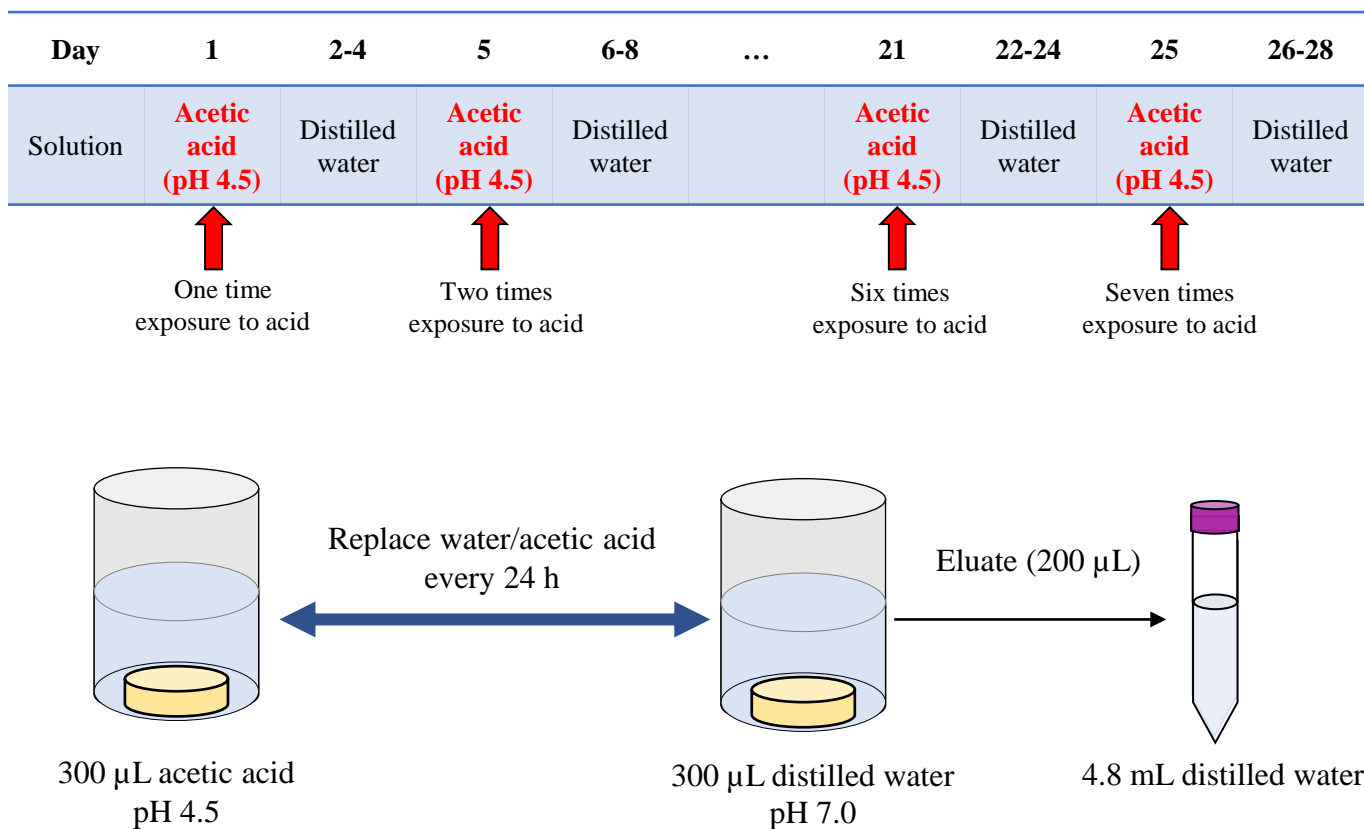


Figure 13. The protocol for measurement of Zn^{2+} release from CA with repeated expose to acid.

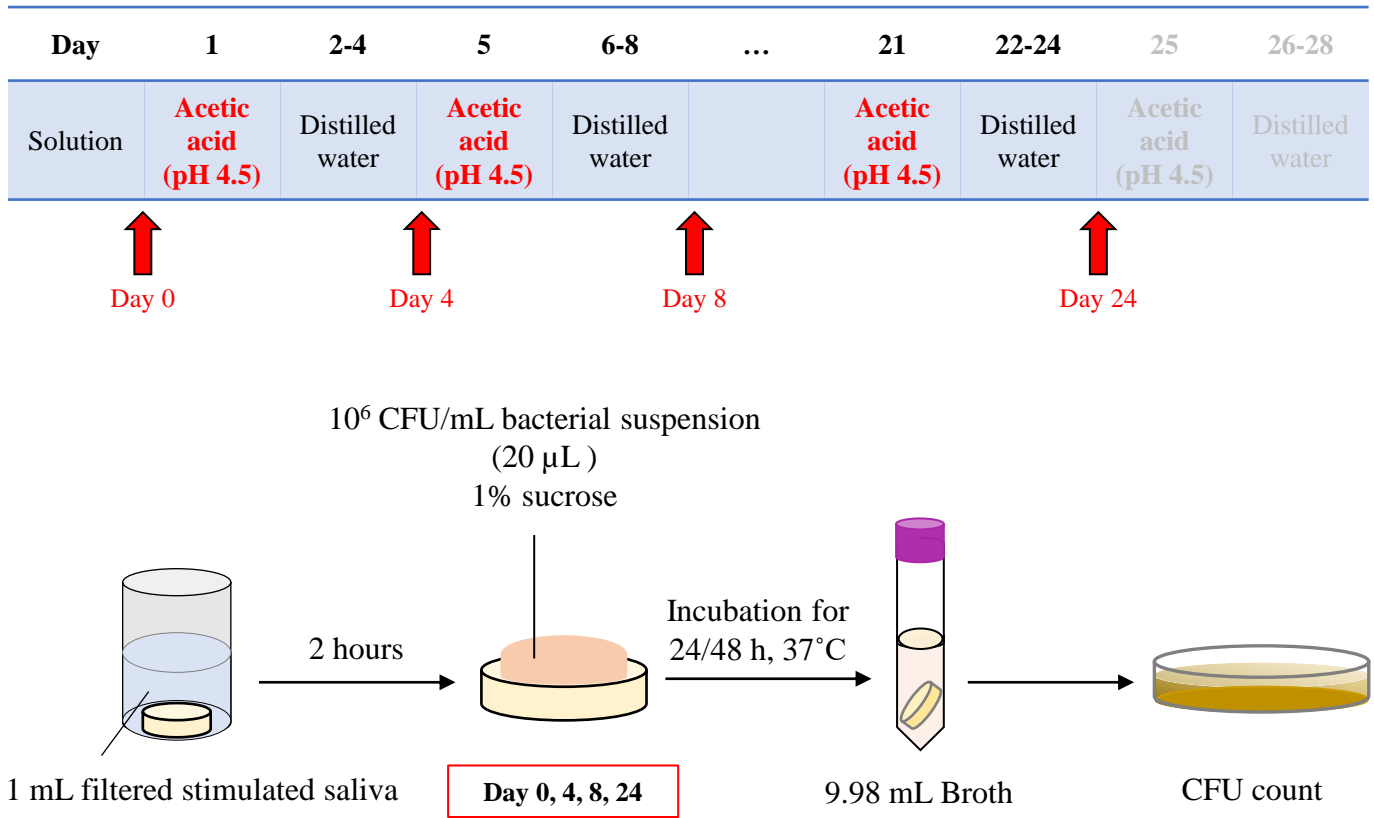


Figure 14. The protocol for antibacterial activity test of CA with repeated expose to acid.

Set specimens

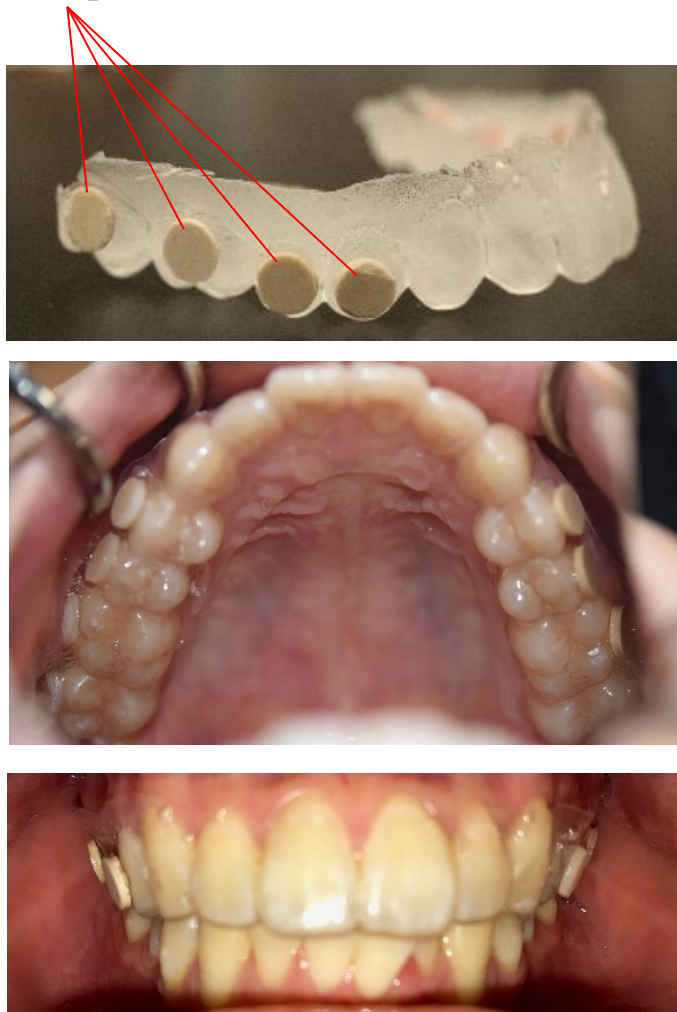


Figure 15. Custom-made splint and disc-shaped specimens for *in situ* assessments.

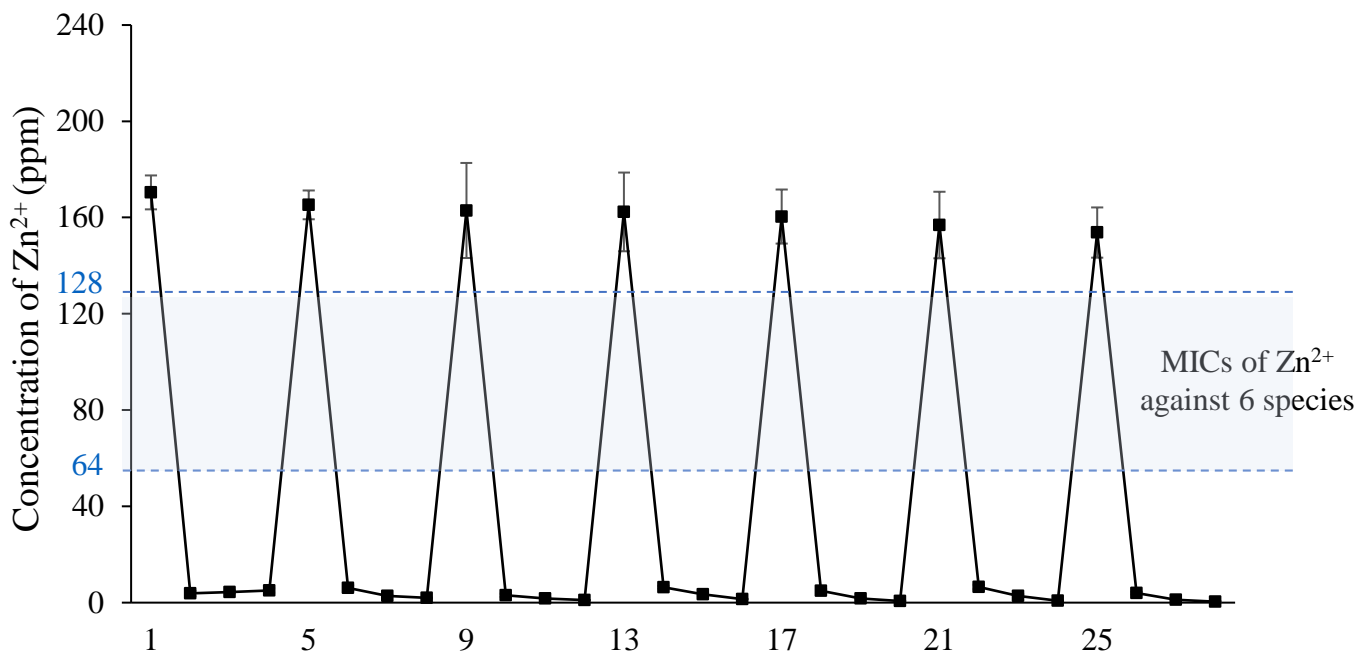


Figure 16. Release profile of Zn²⁺ from CA after repeated exposure to acetic acid.

The bars represent the standard deviations of five replicates.

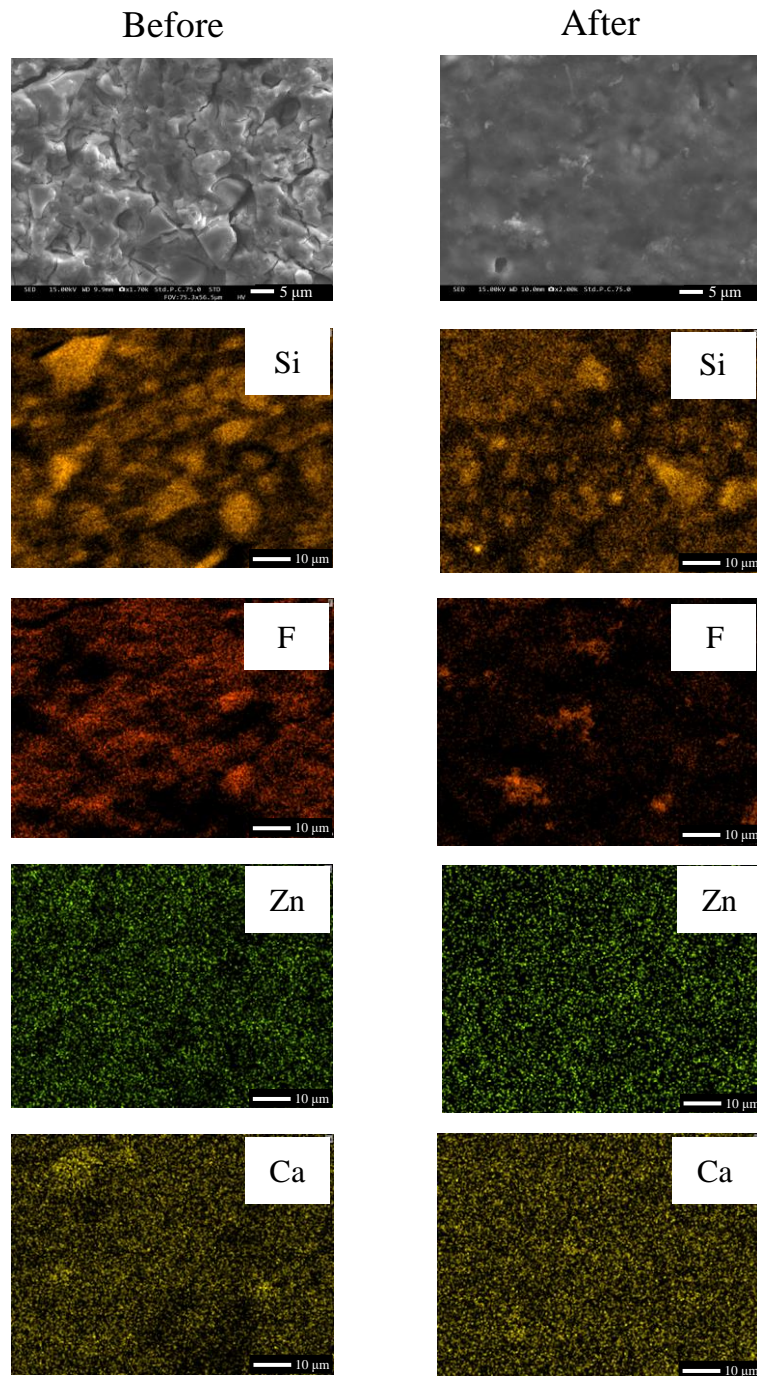


Figure 17. FE-SEM images and elemental mapping images of CA before and after repeated exposure to acetic acid.

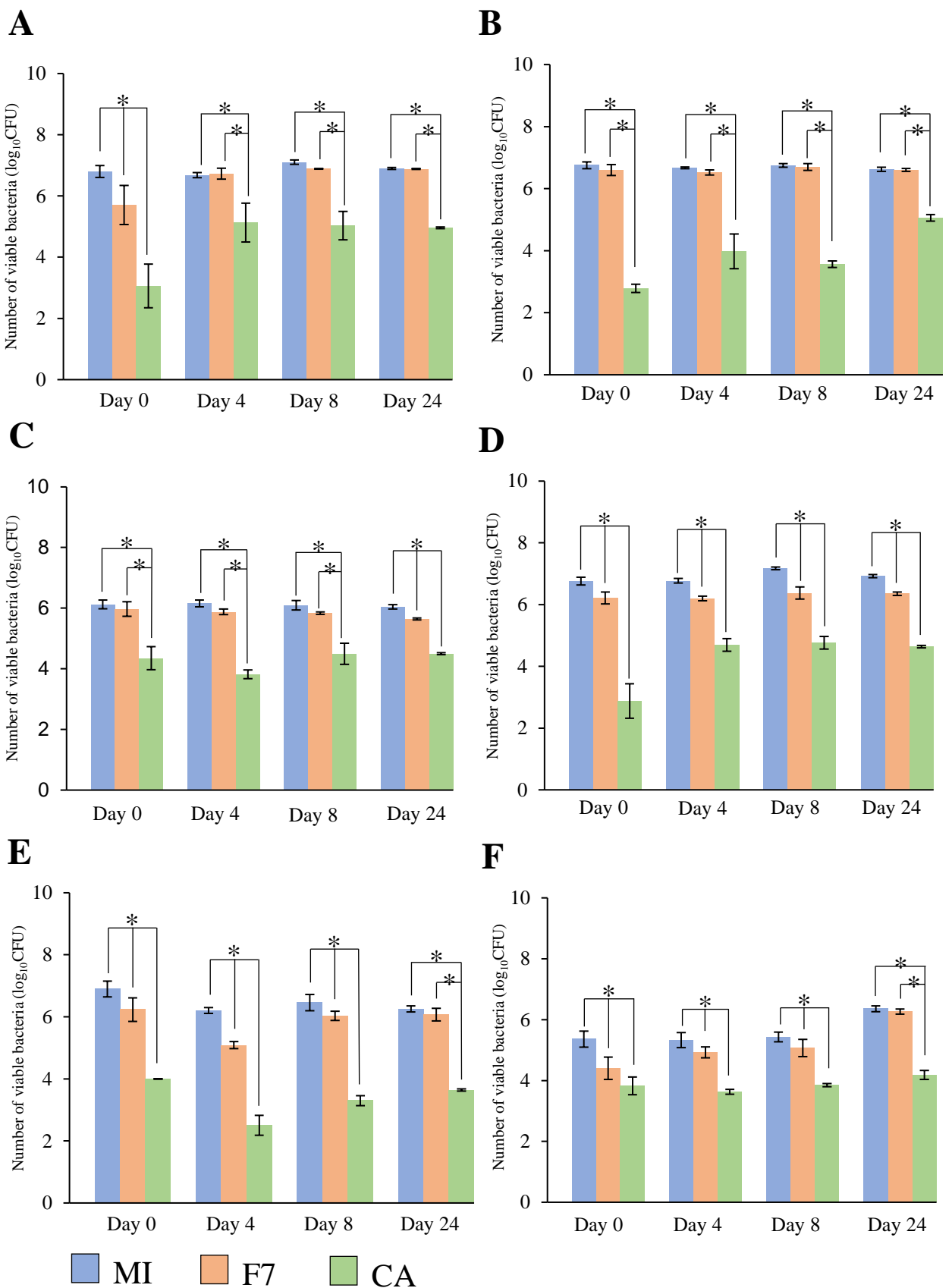


Figure 18. Inhibitory effects of CA before and after repeated exposure to acid against the growth of (A) *S. mutans*, (B) *S. sobrinus*, (C) *S. oralis*, (D) *S. mitis*, (E) *A. naeslundii*, and (F) *F. nucleatum*.

The bars represent the standard deviations of five replicates. * indicates significant differences ($p < 0.05$, ANOVA, Tukey's HSD test).

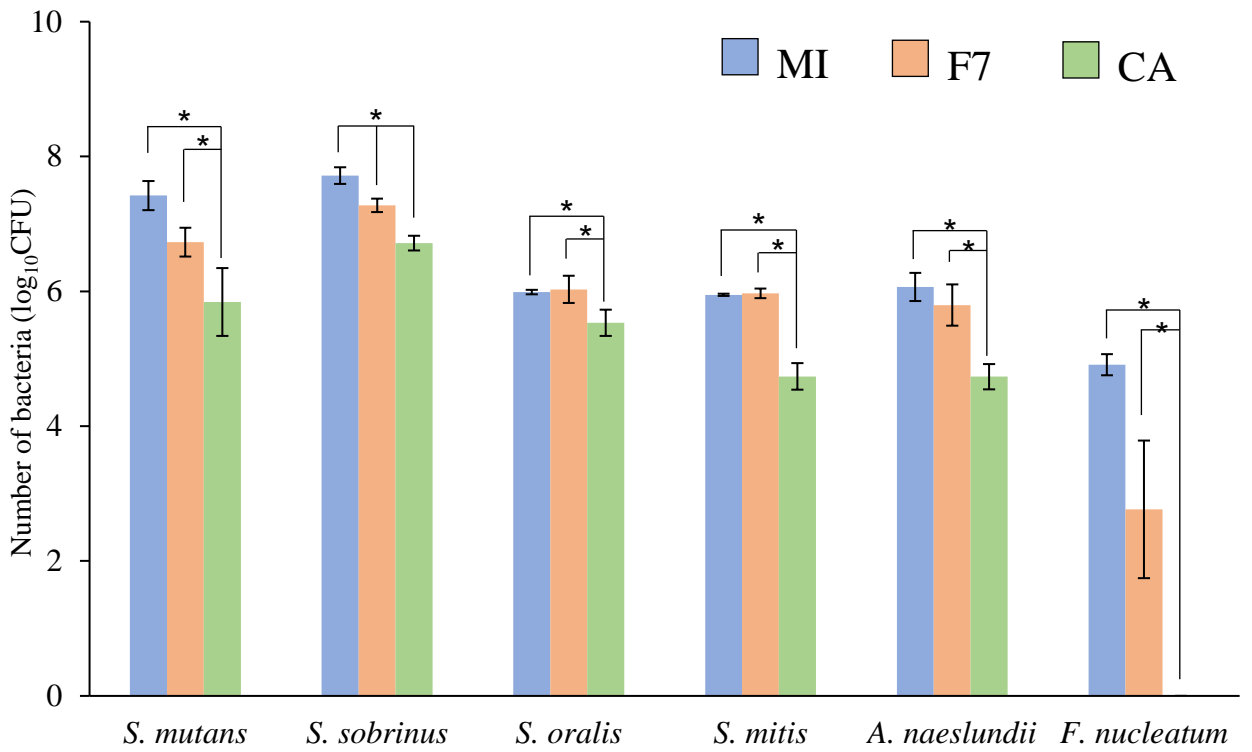
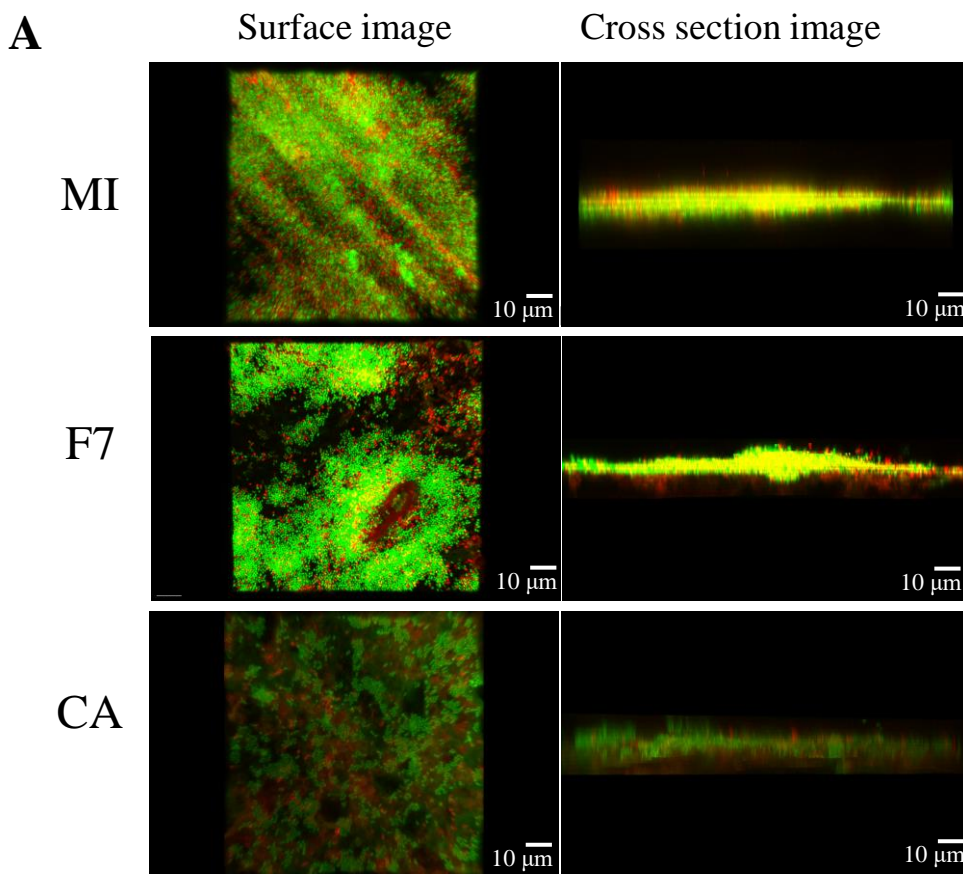
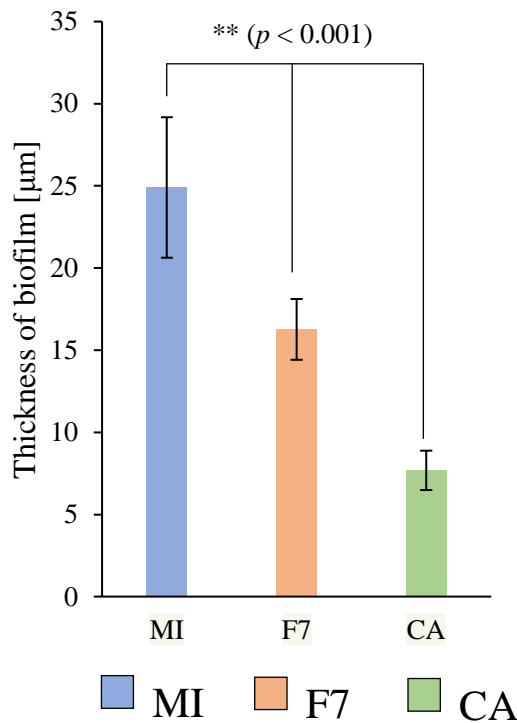


Figure 19. Number of bacteria adhered on the set specimens after incubation for the six bacterial species.

The bars represent the standard deviations of five replicates. * indicates significant differences ($p < 0.05$, ANOVA, Tukey's HSD test)



B



C

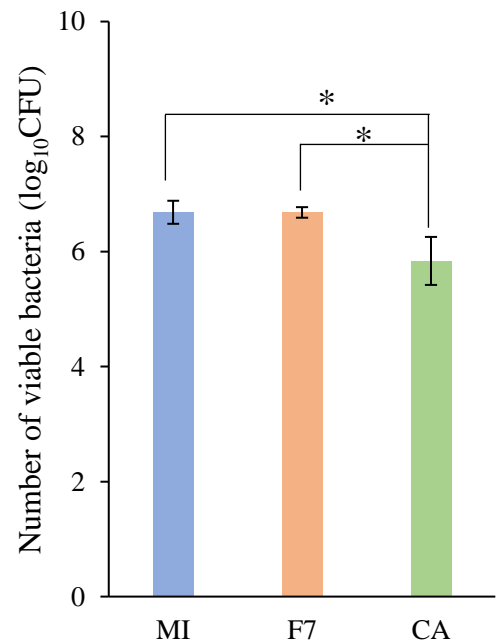


Figure 20. *In situ* biofilm formation on the surface of each specimen.

A: CLSM images. B: Thickness of biofilm analyzed from CLSM images. C: The number of surviving cells in the biofilm. The bars represent the standard deviations of four replicates.

** indicates significant differences ($p < 0.001$, ANOVA, Tukey's HSD test).

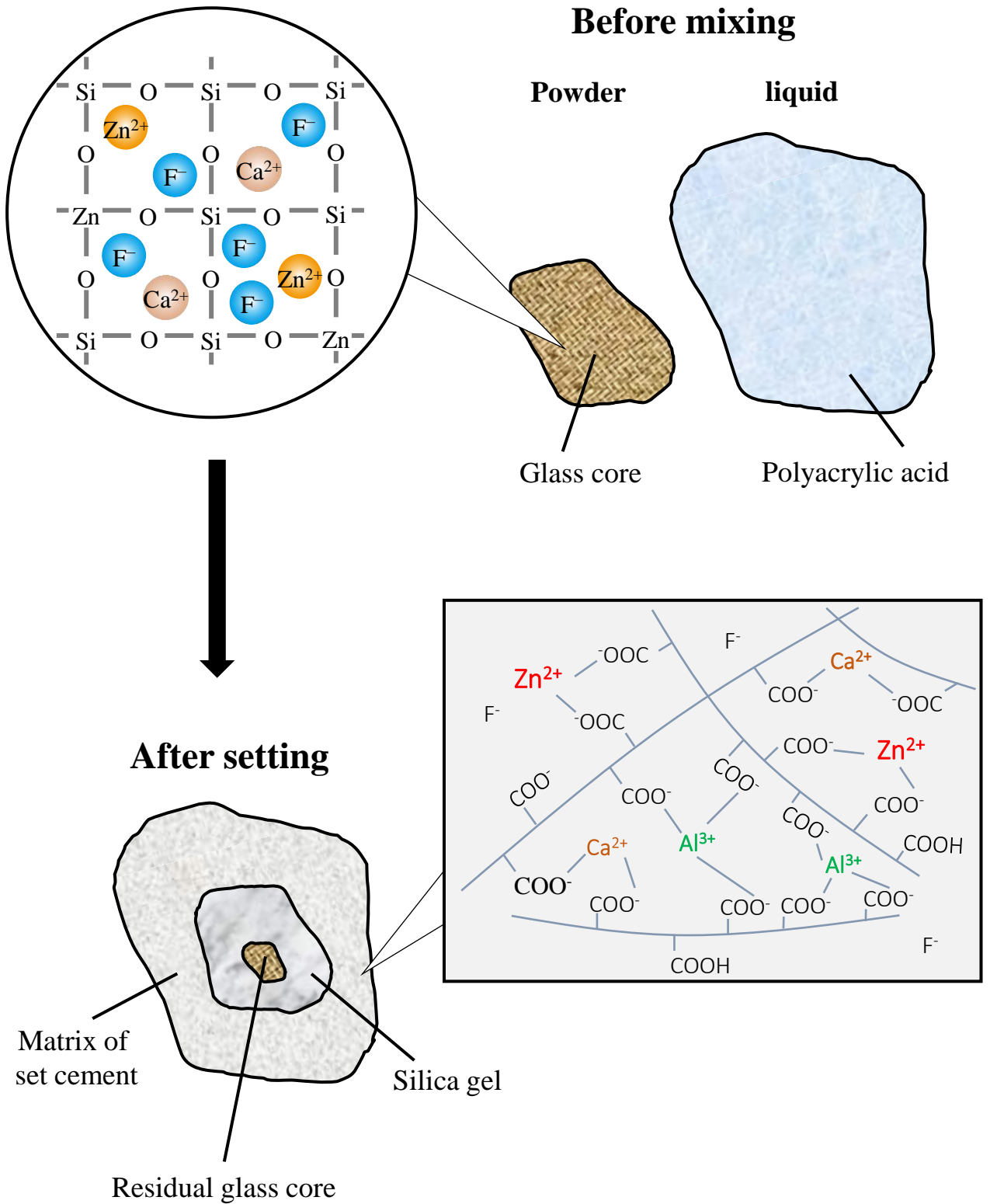


Figure 21. Schematic diagram of reaction of BU in the powder of CA with polyacrylic acid.